UNIVERSITAT DE BARCELONA

Hole dynamics in one-dimensional optical lattices

Author:

David Ribes Marzá

Supervisors:

Ivan Morera, Grigory Astrakharchik

A MASTER THESIS FOR

MASTER IN QUANTUM SCIENCE AND TECHNOLOGY

University of Barcelona, July 2023

Abstract

We study the dynamical properties of a single hole on top of a Mott insulator described by the Bose-Hubbard Hamiltonian in the strongly interacting regime. The full Hamiltonian can be mapped to an effective one by means of the perturbation theory approach, which allows us to obtain the hole effective mass and study the long-time dynamics of a hole, initially localized with a Gaussian distribution or a delta function. The hole effective mass becomes infinite at a critical value of the on-site interaction, which is reflected in its time evolution described by a dispersionless Gaussian distribution. Moreover, a hole, initially localized in a single site, exhibits an oscillatory behavior in its time evolution. We also perform exact diagonalization simulations of the full Bose-Hubbard model and compare the results with the predictions obtained with perturbation theory. The hole effective mass shows a similar trend in the strong coupling regime as in our perturbation theory, however, it does not diverge at a critical on-site interaction. Nevertheless, we also obtain an oscillatory behavior of the hole density in time when starting the time evolution with a hole localized in a site.

Keywords: Effective Hamiltonian, Effective mass, Quasimomentum, Hole

Contents

Acknowledgements

I would like to thank Ivan Morera for his constant help and guidance along the whole thesis. His support and concern for this work have given me a very pleasant research experience. I also want to acknowledge Profs. Grigory Astrakharchik and Bruno Juliá-Díaz for their ideas, suggestions and encouragement. Moreover, thanks to Abel Rojo, for his help with Python and computational methods.

Finally, I want to thank my brother Albert, for his help, and Hanna, for her support and corrections.

1 Introduction

Understanding properties of materials and their main features from a microscopic scale is crucial to develop new quantum technologies [ABB+18]. In the last decades there have been tremendous efforts to give theoretical comprehension of exotic phases of matter such as superconductivity [BCS57], superfluidity [Kap03] or the insulating phase [Koh64]. Experimental studies need to be performed to verificate theoretical predictions [FK07, AEM+95, BSH97, BSTH95, DMA+95, FKW+98]. Nevertheless, since quantum simulators are used to make predicitons as well, their use has vastly increased in the last years. Some examples of quantum simulators are trapped ions [BCMS19, HJG+98], superconducting qubits [DWM04, HWFZ20] and ultracold atoms [SFS+20, LSA+07]. The latter allows the study of both bosonic and fermionic systems in optical lattices described by the Ising and Hubbard models, among others. Using ultracold atoms it is possible to study several phenomena such as Mott-superfluid quantum phase transition [GME+02], Bose-Einstein condensation [AEM+95], quantum magnetism [WHR15] or superfluidity [Zwi14].

The comprehension of the behavior of some materials is significantly influenced by the presence of a certain amount of dopants within them. Holes become a relevant entity when describing superfluids and superconductors [AKL+17, BHB+22, BHR+21]. The mechanism of hole pairing in two-dimensional lattices with fermionic atoms arranged in an antiferromagnetic order underlies unconventional superconductivity [HCB+23, LGSV98, BDG22, SSBG23]. Moreover, hole dopants also dictate magnetic correlations of a strongly interacting fermionic system with specific lattice geometries and temperature of the order of the hopping strength [MKNS+23, MBHD21]. In a triangular lattice, a hole-doped system presents antiferromagnetic correlations given by charge carriers propagating in a spin incoherent Mott insulator. Such carriers, which can also be defined as antiferromagnetic polarons, are originated by the kinetic frustration of single holes [MKNS+23, MBHD21]. On the other hand, it has been experimentally proved that doping with holes a fermionic system in a two-dimensional square lattice results in a reduction of the staggered magnetization of the system, which quantifies the global antiferromagnetic order [MCJ+17]. For hole doping values of about 15%, antiferromagnetic long range order vanishes [MCJ+17].

In this work we investigate a zero temperature bosonic system allocated in a one-dimensional optical lattice. In Sec. 2 we introduce the Bose-Hubbard Hamiltonian that describes our system and the two methods we use to extract the main properties of it, exact diagonalization (ED) and perturbation theory. In Sec. 3, we discuss the different regimes of the Hamiltonian based on the strength of the interaction between bosons: the non-interacting limit, the infinite interaction or Tonks-Girardeau limit, and the strongly interacting regime. Additionally, we introduce holes as quasiparticles and compute an effective Hamiltonian that gives an accurate description of the full Hamiltonian if the interaction strength is much larger than the hopping strength of the bosons. In Sec. 4.1 and 4.2 we use the effective Hamiltonian and the full Hamiltonian respectively to examine the effective mass of a single hole in the system and its dynamics along the lattice. From our results one can quantitatively evaluate in which regimes the effective Hamiltonian describes the main features of the system given by the Bose-Hubbard Hamiltonian. Finally, we summarize our results and display the main conclusions of the work in Sec. 5.

2 Model and methods

2.1 Model

We study an ultracold bosonic system in a one-dimensional periodic optical lattice [LSA+07], which is sufficiently high so that particles' location can be described by discrete positions called lattice sites, which are distanced from each other by the lattice spacing a, fixed to 1 in this work. A Hamiltonian that describes such system is the Bose-Hubbard Hamiltonian,

$$\hat{H} = -J\sum_{i=1}^{N_s}\left[\hat{b}_i^\dagger\hat{b}_{i+1} + \text{h.c.}\right] + \frac{U}{2}\sum_{i=1}^{N_s}\hat{n}_i(\hat{n}_i - 1) = \hat{H}_J + \hat{H}_U. \tag{1}$$

Here, N_s is the number of sites in the lattice, $\hat{b}_i^\dagger$ and $\hat{b}_i$ are operators which create and annihilate a boson at site i, and $\hat{n}_i = \hat{b}_i^\dagger\hat{b}_i$ is the number operator. The factor J is the tunneling amplitude between two neighboring sites (the so-called kinetic, hopping or tunneling term) which we consider to be positive, and U is the on-site interaction strength (short-range interaction). If the interaction between two bosons is attractive, then $U < 0$, which makes the system reduce its energy when they are in the same site. On the contrary, if the interaction is repulsive, $U > 0$.

In this work we mostly focus on the system in the vicinities of the Mott insulator phase, where the interaction repulsive term is much larger than the hopping term ($|U| > J$). In addition, we work in the canonical ensemble, where the total number of particles is a fixed value and thus, the number operator can be substituted by this value, $\hat{N} = \sum_{i=1}^{N_s}\hat{n}_i = N$. Specifically, we work with $N = N_s - 1$, which makes the system having at least one non-occupied site. We refer to this lattice site as the hole.

2.2 Methods

There are different approaches that can be used to tackle the ground state properties of the system we want to study. Among them, there is the tensor networks approach of density matrix renormalization group (DMRG)[Whi92, Whi93, WF04, Sch11], quantum Monte Carlo methods (QMC) [Ast14, MDK+11, CSPS07, CSSPS08, FCM+11, ZKKT09] and the one we are using in this work, ED [ZD10, RGLJD17] (performed with the Python programming language).

The ED method is based on the construction of a Fock basis which defines states that are modified by operators involved in the Hamiltonian, in our case, creation and annihilation operators. The Fock basis one needs to work with depends on two parameters, the number of lattice sites and the number of particles. To define a Fock state, we first create an array of length N_s, the number of lattice sites. Each element of this array corresponds to a certain lattice site, and its value corresponds to the amount of bosons located in the site. As an example, if we have a lattice of $N_s = 3$ and two bosons located in the first and last site, we can represent the Fock state $|1, 0, 1\rangle$ as

```
state = np.array([1,0,1]).
```

With this method we create the Fock basis with a series of routines that create all the possible combinations of particles distributions in a lattice (see Appendix A.1). Moreover, we also define creation and annihilation operators to create the Hamiltonian we work with

(see Appendix A.2).

One of the greatest inconveniences of the ED method is that the size of the Hilbert space increases exponentially fast with the number of sites and particles. It is not just a matter of computation time, but also about memory capacity. To be more specific, the size of the Hilbert space of a system with N_s lattice sites and N identical bosons is $\binom{N+N_s-1}{N} \times \binom{N+N_s-1}{N}$ wich, for the case of $N_s = 10$, $N = 9$, becomes 48620×48620.

To deal with time and memory capacity issues, we combine ED with the analytical approach of perturbation theory. This method assumes that one of the factors of the Bose-Hubbard Hamiltonian, the hopping term $\hat{H}_J$, is much smaller than the on-site interaction term $\hat{H}_U$, which tranlates into $J/|U| \ll 1$. With this approach it is possible to obtain a certain manifold of the energy spectrum of the Hamiltonian. Details on the perturbation theory method can be found in Sec. 3.3.

3 The Bose-Hubbard model

As we have seen in Eq. 1, the Bose-Hubbard Hamiltonian consists of two terms, the hopping and the on-site interaction terms. The main feature of the model is the competition between the kinetic energy driven by the tunneling factor J and the contact interaction energy U. The first term allows the bosons to be delocalized in the lattice and make the ground state be in a superfluid phase [Leg99, RB03, JBC+98], which is characterized by a quasi long-range phase coherence, among others. When the interaction term dominates, a Mott insulator phase is formed, which is characterized by a localization of the bosons in the lattice sites and a reduction of the local particle number fluctuations [JBC+98]. The presence of a superfluid phase and a Mott insulator phase yields to the existance of a quantum phase transition, which is found at ratio $J/U \approx 0.3$ in one-dimensional systems [KWM00]. In this section we study the main features of the Hamiltonian in different limits by modifying both the on-site interaction U and the kinetic term J.

3.1 Non-interacting limit. $U = 0$

The non-interacting limit corresponds to considering a vanishing on-site interaction potential, $U = 0$. This case can be analytically solved for any number of sites and particles performing a Fourier transform of the operators (see Appendix B for a detailed calculation) to write the Hamiltonian in the momentum space. Note that this transformation is only valid in a system with periodic bounday conditions [Mis12]. The new Hamiltonian in momentum space reads

$$\hat{H}_q = -2J \sum_q \hat{n}_q \cos q, \tag{2}$$

where q is the quasimomentum of a particle and $\hat{n}_q$ the number operator in momentum space, which counts the occupation number of the state with quasimomentum q. Since the Hamiltonian is diagonal in this basis, it is straightforward to obtain the different energy levels of the spectrum. The ground state sets all the bosons in the system with a quasimomentum $q = 0$. Hence, its energy reads $E_0 = -2JN = -2J(N_s - 1)$.

The first excited state is that with a boson promoted to the next q value, in an increasing order of $|q|$, which is $q = \pm\frac{2\pi}{Ns}$ [Mis12]. Since the dispersion relation from

Eq. 2 is an even function, this state will be doubly degenerate. Its energy reads $E_1 = -2J(N - 1 + \cos\frac{\pm 2\pi}{N_s}) = -2J(N_s - 2 + \cos\frac{\pm 2\pi}{N_s})$.

In a general form, all eigenvalues can be written as a sum of single particle dispersion relations

$$E = \sum_{i=1}^{N} -2J\cos q_i, \quad q_i = \frac{2\pi}{N_s}k \begin{cases} k = 0, \pm 1, \pm 2, ..., -\dfrac{N_s}{2} & \text{for } N_s \text{ even}, \\ k = 0, \pm 1, \pm 2, ..., \pm\dfrac{N_s - 1}{2} & \text{for } N_s \text{ odd}, \end{cases} \tag{3}$$

where q_i is the quasimomentum of the i-th particle, which is discretized in units of $2\pi/N_s$.

3.2 Tonks-Girardeau limit. $U \to \infty$

A positive value of the on-site interaction U corresponds to a repulsive behavior between bosons in the lattice. When this parameter becomes very large, configurations with more than one boson per site are suppressed, which means that the bosons in the lattice become impenetrable and can be treated as hard-core bosons.

Hard-core bosons are particles that follow bosonic statistics but have a fermionic-like behavior, two of them cannot occupy the same lattice site. We define new operators $\hat{a}_i^\dagger$ and $\hat{a}_i$, which create and annihilate these new particles at site i. Since these operators are a crossover between bosons and fermions, they have mixed commutation and anticommutation relations, $[\hat{a}_i, \hat{a}_j^\dagger] = [\hat{a}_i, \hat{a}_j] = [\hat{a}_i^\dagger, \hat{a}_j^\dagger] = 0$ for $i \neq j$, $\{\hat{a}_i, \hat{a}_i^\dagger\} = 1$ and $(\hat{a}_i)^2 = (\hat{a}_i^\dagger)^2 = 0$ [CLRS11]. Then we rewrite the Hamiltonian with these new operators by associating $\hat{b}_i \leftrightarrow \hat{a}_i$ and $\hat{b}_i^\dagger \leftrightarrow \hat{a}_i^\dagger$, which yields

$$\hat{H} = -J\sum_{i=1}^{N_s}\left[\hat{a}_i^\dagger\hat{a}_{i+1} + \text{h.c.}\right] + \frac{U}{2}\sum_{i=1}^{N_s}\hat{a}_i^\dagger\hat{a}_i(\hat{a}_i^\dagger\hat{a}_i - 1). \tag{4}$$

After some mathematical manipulations using the mixed commutation and anticommutation relations of hard-core bosons operators, the on-site interaction term vanishes. To proceed now, we perform a transformation to "fermionize" the hard-core bosons by modifying the operators into fermionic ones. The transformation between these two operators is the Jordan-Wigner transformation [JW28], and reads

$$\begin{aligned} \hat{a}_j &= (-1)^{\sum_{i<j}\hat{n}_i}\hat{c}_j, \\ \hat{a}_j^\dagger &= (-1)^{\sum_{i<j}\hat{n}_i}\hat{c}_j^\dagger. \end{aligned} \tag{5}$$

Substituting these operators in the original Hamiltonian with the vanished on-site interaction results in a simple hopping Hamiltonian for fermions, which can be solved again in the momentum space, (see Appendix B)

$$\hat{H}_q = -2J\sum_q \hat{n}_q\cos q. \tag{6}$$

Note now that from a mathematical perspective, our system has become fermionic. This means that the ground state is not anymore that with all particles with $q = 0$, since two identical fermions cannot occupy the same quasimomentum state. In fact, the ground state will be that with all momenta filled until the last particle of the system has the

maximum quasimomentum, the so-called Fermi momentum q_F. Its value can be related to the number of lattice sites through the expression $q_F = \frac{2\pi}{N_s}\mathcal{L}$, where $\mathcal{L} = \frac{N}{2}$ for N even, and $\mathcal{L} = \frac{N-1}{2}$ for N odd. Hence, all occupation numbers of momentum up to the Fermi momentum will be one: $\hat{n}_q = 1$ for $|q| \leq q_F$. The ground state energy of this system corresponds to the Fermi sea, and reads [Kru16] (see Appendix C for a detailed derivation)

$$E_0 = -2J\sum_q \cos q = -2J\frac{\sin\left(\frac{\pi N}{N_s}\right)}{\sin\left(\frac{\pi}{N_s}\right)} = -2J\frac{\sin\left(\frac{\pi(N_s-1)}{N_s}\right)}{\sin\left(\frac{\pi}{N_s}\right)}. \tag{7}$$

The ground state of this system is trivially written, in momentum space and fermionic operators (note that the actual system is bosonic, thus, it can be written with bosonic operators using the Jordan-Wigner transformation),

$$|\psi\rangle = \prod_{|q|\leq q_F} \hat{c}_q^\dagger |0\rangle . \tag{8}$$

3.3 Strongly interacting regime. $J/U \ll 1$

We now consider the system with a strong but finite on-site interaction, where bosons are penetrable (but still repulsive) and a single site can be occupied by more than one boson at an energetic cost of U. We use the method of perturbation theory, which allows us to obtain a good approximation of the energy levels in the first manifold.

In the system we are studying, where $N = N_s - 1$, manifolds are distinguished between each other by the amount of boson pairs that occupy the same site. Hence, the lowest manifold is that with no pairs in the same site, which we refer to as the "hard-core bosons manifold". The next manifold has one pair of bosons in the same site, and so on. Since we want to study the ground state of the system, we restrict our system to the hard-core bosons manifold.

Assuming $J \ll |U|$, the hopping term $\hat{H}_J$ corresponds to the perturbative Hamiltonian while the on-site interaction term $\hat{H}_U$ is the non-perturbed Hamiltonian, whose eigenvalues and eigenvectors are known (it is diagonal). It is clear that the spectrum of $\hat{H}_U$ is degenerate. The eigenvalue $E = 0$ is degenerate as many times as the number of combinations of N particles in N_s sites without placing more than one particle in each site. The next eigenvalue, $E = U$, is degenerate as many times as the number of combinations of N particles in N_s sites by having one single site with two particles, and the rest with one particle. Knowing this, we use degenerate perturbation theory to obtain an approximate solution of Bose-Hubbard Hamiltonian (see Appendix D.1 for a detailed example).

Since we work in the hard-core bosons manifold, we use a special notation for the Hilbert space basis. The label of every state is the number corresponding to the lattice site where there is no boson (note that in this manifold, for $N = N_s - 1$, there is just one). We refer to this empty lattice site as the hole. Thus, the notation reads

$$|3\rangle = |1,1,0,1,1,1...,1\rangle , \quad |5\rangle = |1,1,1,1,0,1,1...,1\rangle . \tag{9}$$

Using this basis, an effective Hamiltonian describing the system can be written in matrix form (see Appendix D.2 for the derivation in detail)

$$\langle n|\,\hat{H}_{\text{eff}}\,|m\rangle = -J(\delta_{n,m-1}+\delta_{n,m+1}) - 2(N_s-2)\frac{2J^2}{U}\delta_{n,m} - \frac{2J^2}{U}(\delta_{n,m-2}+\delta_{n,m+2}). \quad (10)$$

Note that the size of this new Hamiltonian matrix is $N_s \times N_s$ which is much smaller than the original Bose-Hubbard Hamiltonian. Hence, now it is possible to perform exact diagonalization for a system with a larger number of lattice sites. In Fig. 1 we present a comparison of the ground state energy and the computation time between both Hamiltonians.

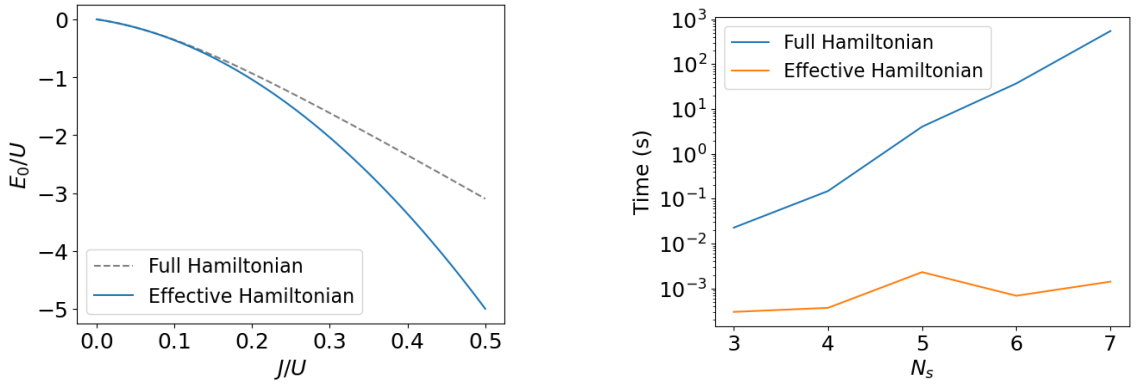

(a) (b)

Figure 1: **(a)** Ground state energy of the system in units of U as a function of J/U for $N_s = 5$, $N = 4$ and periodic boundary conditions. Up to $J/U = 0.2$, the effective Hamiltonian obtained with perturbation theory gives a very accurate result. **(b)** Computation time of ED with both full and effective Hamiltonian as a function of N_s, the size of the lattice. The total number of particles is fixed to $N = N_s - 1$.

The perturbation theory approach is also valid when the system is strongly attractive, $|U| \ll J$. In such case, the obtained manifold is not that with the lowest energy, but the one with the highest. Notice also that both the Full Bose-Hubbard Hamiltonian and the effective Hamiltonian fulfill the symmetry $\hat{H}(U) = -\hat{H}(-U)$ if N_s is even and the system has periodic boundary conditions [LZ09] (see appendices E.1 and E.2 for derivation and details). This symmetry indicates that the ordering of the spectrum for $U > 0$ is inverted with respect that of $U < 0$. We analyze the spectrum in both regimes and compare them with the result obtained from the full Bose-Hubbard Hamiltonian in Fig. 2.

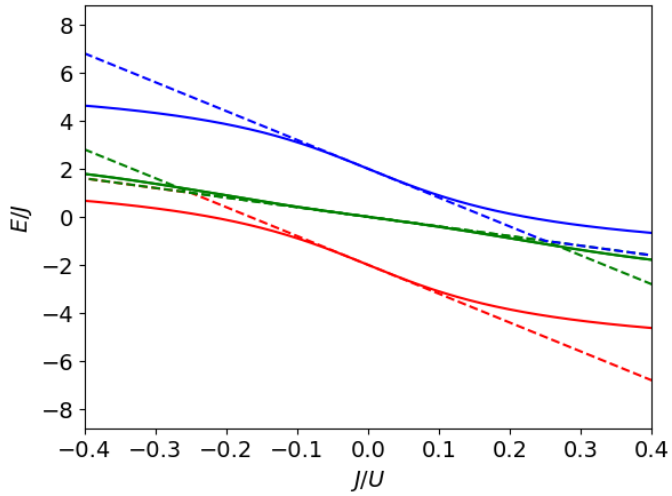

Figure 2: Energy spectrum of both effective Hamiltonian (dashed lines) and full Hamiltonian (solid lines) as a function of J/U for $N_s = 4$, $N = 3$ and periodic boundary conditions. The hopping amplitude is fixed at $J = 1$ and U is modified along the horizontal axis. When U is positive, the ground state (red line) and the three next excited states are plotted. When U is negative, they are not the lowest energy states, but the highest ones of the spectrum, since the plotted manifold is that of hard-core bosons. The symmetry $\hat{H}(U) = -\hat{H}(-U)$ is observed since, for every eigenvalue at a certain U with $E(U)$, exists a partner eigenvalue with $-E(-U)$. Up to a ratio of $J/U = 0.2$, the effective Hamiltonian leads to a very accurate result. While the different eigenstates cross each other in the effective Hamiltonian, they do not in the full Bose-Hubbard Hamiltonian.

3.3.1 Effective Hamiltonian in operator form

The Hamiltonian represented by the matrix elements in Eq. 10 can be written in operator form, which leads to an explicit description of the physical processes occurring in the system. In this section we present its derivation as well as a description of its main features.

We first need to obtain the effective Hamiltonian written in hard-core bosons operators for an arbitrary number of particles N, which reads (see Appendix D.3 for further details)

$$\hat{H}_{\text{eff}} = -J \sum_{i}^{N_s} \left[\hat{a}_i^\dagger \hat{a}_{i+1} + \text{h.c.}\right] - \frac{4J^2}{U} \sum_{i}^{N_s} \hat{n}_i \hat{n}_{i+1} - \frac{2J^2}{U} \sum_{i}^{N_s} \left[\hat{a}_{i-1}^\dagger \hat{n}_i \hat{a}_{i+1} + \text{h.c.}\right]. \tag{11}$$

The first term describes a first neighbors hopping process of a particle (note that, since $\left(\hat{a}_i^\dagger\right)^2 = 0$, the hopping of a particle to an occupied site is not allowed, yielding to the vanishing of such term). The second term, which is analogous to a superexchange process, is an interaction between two particles located in two neighboring lattice sites, its strength is $4J^2/U$. The last term, which has a strength of $2J^2/U$, is a correlated hopping [WK22, Caz03]. It represents an assisted hopping of a hard-core boson to its second neighbor site. It is assisted because it needs a boson in the middle site to be an allowed process, which is ensured by the number operator $\hat{n}_i$.

Since we want to treat holes as quasi-particles, we introduce now the operators $\hat{h}_i^\dagger$ and $\hat{h}_i$, which create and annihilate a hole at site i in a sea of hard-core bosons. The relation between hard-core boson operators and hole operators reads $\hat{h}_i^\dagger \leftrightarrow \hat{a}_i$, $\hat{h}_i \leftrightarrow \hat{a}_i^\dagger$. Thus, taking into account the mixed commutation and anticommutation relations of hard-core

bosons operators, it is clear the hole operators fulfill them as well, $[\hat{h}_i, \hat{h}_j^\dagger] = [\hat{h}_i, \hat{h}_j] = [\hat{h}_i^\dagger, \hat{h}_j^\dagger] = 0$ for $i \neq j$, $\{\hat{h}_i, \hat{h}_i^\dagger\} = 1$ and $(\hat{h}_i)^2 = (\hat{h}_i^\dagger)^2 = 0$. Substituting the hole operators for the hard-core bosons', the Hamiltonian reads

$$\hat{H}_{\text{eff}} = -J \sum_i^{N_s} \left[\hat{h}_i \hat{h}_{i+1}^\dagger + \text{h.c.}\right] - \frac{4J^2}{U} \sum_i^{N_s} \hat{h}_i \hat{h}_i^\dagger \hat{h}_{i+1} \hat{h}_{i+1}^\dagger - \frac{2J^2}{U} \sum_i^{N_s} \left[\hat{h}_{i-1} \hat{h}_i \hat{h}_i^\dagger \hat{h}_{i+1}^\dagger + \text{h.c.}\right]. \quad (12)$$

After some mathematical manipulations using the mixed commutation and anticommutation relations, it reads

$$\begin{aligned} \hat{H}_{\text{eff}} = -J \sum_i^{N_s} \left[\hat{h}_i^\dagger \hat{h}_{i+1} + \text{h.c.}\right] - \frac{4J^2}{U} N_s + \frac{8J^2}{U} \sum_i^{N_s} \hat{h}_i^\dagger \hat{h}_i - \frac{4J^2}{U} \sum_i^{N_s} \left[\hat{h}_i^\dagger \hat{h}_i \hat{h}_{i+1}^\dagger \hat{h}_{i+1}\right] \\ - \frac{2J^2}{U} \sum_i^{N_s} \left[\hat{h}_{i+1}^\dagger \hat{h}_{i-1} + \text{h.c.}\right] + \frac{2J^2}{U} \sum_i^{N_s} \left[\hat{h}_{i+1}^\dagger \hat{h}_i^\dagger \hat{h}_i \hat{h}_{i-1} + \text{h.c.}\right]. \end{aligned} \quad (13)$$

For our specific system, where there are $N = N_s - 1$ particles and hence, a single hole, several terms can be simplified. While the sum in the third term becomes 1, the fourth and last terms vanish since they describe interactions and asisted hoppings between two holes respectively. Thus, the final Hamiltonian written with hole operators for our case reads

$$\hat{H}_{\text{eff}} = -J \sum_i^{N_s} \left[\hat{h}_i^\dagger \hat{h}_{i+1} + \text{h.c.}\right] - \frac{4J^2}{U}(N_s - 2) - \frac{2J^2}{U} \sum_i^{N_s} \left[\hat{h}_{i-1}^\dagger \hat{h}_{i+1} + \text{h.c.}\right], \quad (14)$$

where the first term represents a first neighbor hopping of the hole, the second term is an N_s-dependent shift in energy, and the last term describes a hopping to second neighbors of the hole.

It is possible to analytically solve this Hamiltonian by writing it in momentum space using the Fourier transform (see Appendix B, which is the analogous process with $\hat{b}$ operators). The new Hamiltonian in momentum space is diagonal and reads

$$\hat{H}_{\text{eff}} = -2J \sum_q \hat{h}_q^\dagger \hat{h}_q \cos q - \frac{4J^2}{U}(N_s - 2) - \frac{4J^2}{U} \sum_q \hat{h}_q^\dagger \hat{h}_q \cos 2q. \quad (15)$$

Since there is a single hole in the system, the sum over the hole occupation number becomes one. Hence, a single hole with quasimomentum q follows the dispersion relation

$$E_{hole} = -2J \cos q + \frac{8J^2}{U} - \frac{4J^2}{U} N_s - \frac{4J^2}{U} \cos 2q. \quad (16)$$

From the dispersion relation plot in Fig. 3 we see that, if the quasimomentum of a hole increases, its energy increases as well and vice versa (as long as $|U| \gg J$). This is, whereas a hole with the lowest possible energy has a quasimomentum of $q = 0$, a maximally excited hole has the maximum quasimomentum possible ($q = \pi$ for N_s even and $q = \pi(N_s - 1)/N_s$ for N_s odd). Conversely, for smaller values of $|U|$, the energy of the hole does not grow along the whole first Brillouin zone when its quasimomentum does.

The same problem can be solved using fermionic operators, which shows a shift in quasimomentum $q \to q + \pi$ (details on the fermionic formalism in appendices D.4 and D.5).

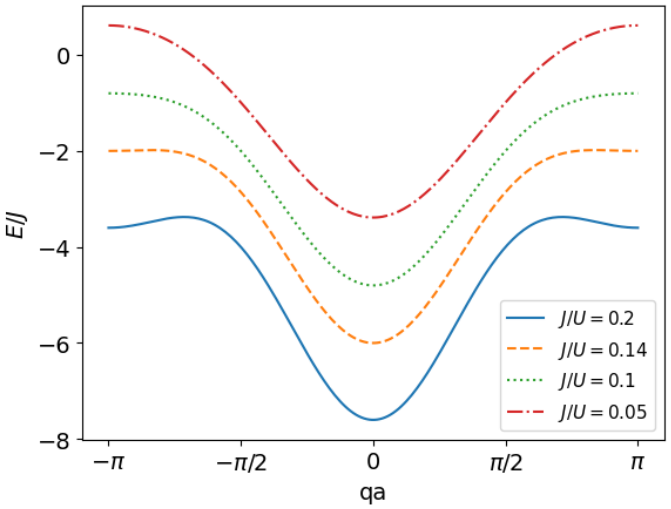

Figure 3: Energy of a hole in units of J as a function its quasimomentum q (known as dispersion relation) for different values of the ratio J/U and $N_s = 8$. The limits of the horizontal axis are given by the frontiers of the first Brillouin zone.

4 Hole dynamics

We have seen that in the limit of $J/|U| \ll 1$, it is possible to describe the hole as a quasiparticle with quasimomentum q which follows the dispersion relation of Eq. 16. We now study the effective mass of the hole. Additionally, we investigate how a localized hole evolves in time for different values of J/U. Moreover, we compare the time evolution obtained with the effective Hamiltonian and the full Bose-Hubbard Hamiltonian.

To analyze how the time evolution changes when the parameters of the Hamiltonian are modified, we fix the tunneling amplitude J to 1 and modify the on-site interaction energy U. Taking this into account, the two critical values at which the masses become infinite for the effective Hamiltonian are $U_c = 8$ and $U_c = -8$. We use this Hamiltonian to perform time evolution of a state with a hole and see how the sign modification of U affects the result. Note that, if we want to investigate how the state changes over time, our initial state cannot be an eigenstate of $\hat{H}$ since its time evolution just adds a non-observable global phase to it. Thus, we apply the time evolution operator $\hat{U}(\hat{H}) = \exp(-i\hat{H}t/\hbar)$ on two different states.

We consider first a state with a fully localized hole in the central lattice site and a single boson in each of the other sites, $|\psi\rangle = |1, ..., 1, 0, 1, ..., 1\rangle$ (note that since the system has periodic boundary conditions, it is translational invariant and thus there is no relevant difference if the hole is located in any other site). The second state we consider is that with a space Gaussian distribution of the hole, centered in the central lattice site. While we time-evolve the first state both with full Bose-Hubbard Hamiltonian and effective Hamiltonian, we time-evolve the second state just with the effective Hamiltonian. The reason for this is that, by simulating the full Hamiltonian with ED, we have a strong limitation in the number of sites due to lack of computation time and memory capacity. To define a smooth Gaussian distribution it is required that the lattice spacing is much smaller than the size of the lattice, hence, a large number of lattice sites N_s is required.

4.1 Effective Hamiltonian

4.1.1 Hole effective mass

From the analytical expression of the dispersion relation of the hole in Eq. 16, it is straightforward to compute the value of the effective mass of the hole, m^*. This result depends on the quasimomentum of the hole, but we will mostly focus on the regions around $q = 0$ and $q = \pi$. The reason for this is that, at those values, the band presents a minimum or maximum, which is where it shows a vanishing linear q dependence for a certain ratio J/U.

To calculate the effective mass at certain q values we expand the dispersion relation in powers of q and identify the kinetic energy $E_q = \hbar^2 q^2/(2m^*)$,

$$\begin{aligned} E_{hole}(q) &\approx -2J - \frac{4J^2}{U}(N_s - 1) + \frac{1}{2}\left(2J + \frac{16J^2}{U}\right) q^2 + \mathcal{O}(q^3) \quad \text{for} \quad q \approx 0, \\ E_{hole}(q) &\approx -2J - \frac{4J^2}{U}(N_s - 1) + \frac{1}{2}\left(\frac{16J^2}{U} - 2J\right) (q - \pi)^2 + \mathcal{O}(q^3) \quad \text{for} \quad q \approx \pi. \end{aligned} \tag{17}$$

Thus, the effective mass at each value of q reads

$$\begin{aligned} \frac{m^*_{q=0}}{\hbar^2} &= \frac{1}{2J + \frac{16J^2}{U}} \approx \frac{1}{2J} - 4\frac{1}{U} + 32\frac{J}{U^2}, \\ \frac{m^*_{q=\pi}}{\hbar^2} &= \frac{1}{\frac{16J^2}{U} - 2J} \approx -\frac{1}{2J} - 4\frac{1}{U} - 32\frac{J}{U^2} \end{aligned} \tag{18}$$

This result indicates that, when the hole has a quasimomentum of $q = 0$, there is a certain critical value of J/U at which the effective mass becomes infinite, this is $J/U = -1/8$. Moreover, when the quasimomentum of the hole is $q = \pi$, the critical value at which the effective mass becomes infinite is $J/U = 1/8$.

4.1.2 Fully localized hole

After having obtained the value of the effective mass of the hole as a function of the energy parameters J and U, we analyze the dynamics of the hole and see how the mass and the time evolution of the state are related. We calculate the time evolution of the hole density ($\hat{\rho}_i = \hat{h}_i^\dagger \hat{h}_i$) expectation value computed with the initially fully localized hole state, here written as $|\psi\rangle$. The analytical expression for this magnitude reads

$$\langle\psi| e^{i\frac{\hat{H}_{\text{eff}}t}{\hbar}} \hat{h}_i^\dagger \hat{h}_i e^{-i\frac{\hat{H}_{\text{eff}}t}{\hbar}} |\psi\rangle . \tag{19}$$

We first analyze the limit of $U \to \infty$. In this regime, the effective Hamiltonian (Eq. 14) becomes a single particle (hole) first neighbors hopping Hamiltonian ($\hat{H}_J$). Thus, the time evolution of the density at the site where the hole is initially located is given by (see apendix F.1 for a detailed calculation),

$$\rho_{i=\frac{N_s}{2}}(t) = J_0^2\left(\frac{2Jt}{\hbar}\right), \tag{20}$$

where J_0 is zeroth order Bessel function of the first kind. This result indicates that the hole density oscillates over time with a decreasing amplitude (see Fig. 4).

Let us now consider the regime of strong but finite interactions within the effective Hamiltonian description. Constant terms can be discarded since they just represent an energy shift, which yields a non-relevant common phase when performing time evolution. Hence, the Hamiltonian from Eq. 14 reduces to a single particle hopping to first and second nearest neighbors with amplitudes J and $2J^2/U$ respectively. The analytical expression for the hole density over time in the initial site becomes now (see Appendix F.2 for detailed calculation),

$$\rho_{i=\frac{N_s}{2}}(t) = \Gamma(t)^*\Gamma(t) = \left| \sum_{n=0}^{\infty} \left(\frac{-i\lambda t}{\hbar} \right)^n \frac{1}{n!} \sum_{k=0}^{n} \binom{n}{k} J_{2|n-2k|} \left(\frac{2Jt}{\hbar} \right) \right|^2 , \tag{21}$$

where $\lambda = 2J^2/U$ is the second neighbors tunneling amplitude, and J_n is the n-th order Bessel function of first kind.

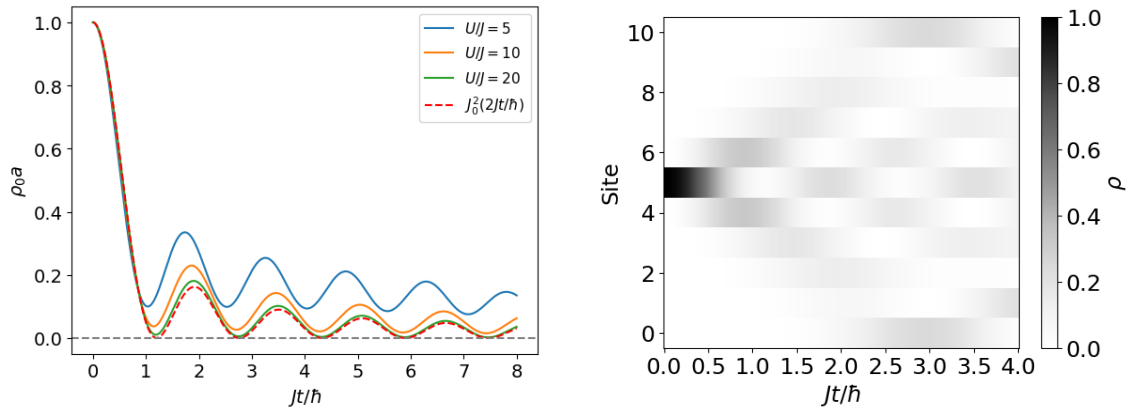

(a) (b)

Figure 4: **(a)** Hole density of central site as a function of $Jt/\hbar$. When $U \to \infty$, the function tends $J_0(2Jt/\hbar)^2$, that obtained for a single particle in an empty lattice. This result does not thake into account the finite size effects of the lattice. **(b)** Hole density evolution over time and lattice site computed with the effective Hamiltonian with $U = 10$. At $Jt/\hbar \approx 3$ the hole wavefront reaches the lattice edge, which indicates that its speed over the lattice is $v \approx 1.66\ \hbar/(Jt)$ for $U = 10$.

The position of the first minimum, here defined as $\rho_0(t_0) = \rho_{\min}$, varies with J/U. When the contact interaction U becomes larger, the minimum tends to that of the Bessel function J_0^2 (single particle case). The presence of a superexchange process in the Hamiltonian based on a mediated hopping to second neighbors can be experimentally captured by measuring the position of the first minimum in the density over time. If the density strictly vanishes at $2Jt/\hbar \approx 2.4$, the Hamiltonian does not present a superexchange process, otherwise, it does.

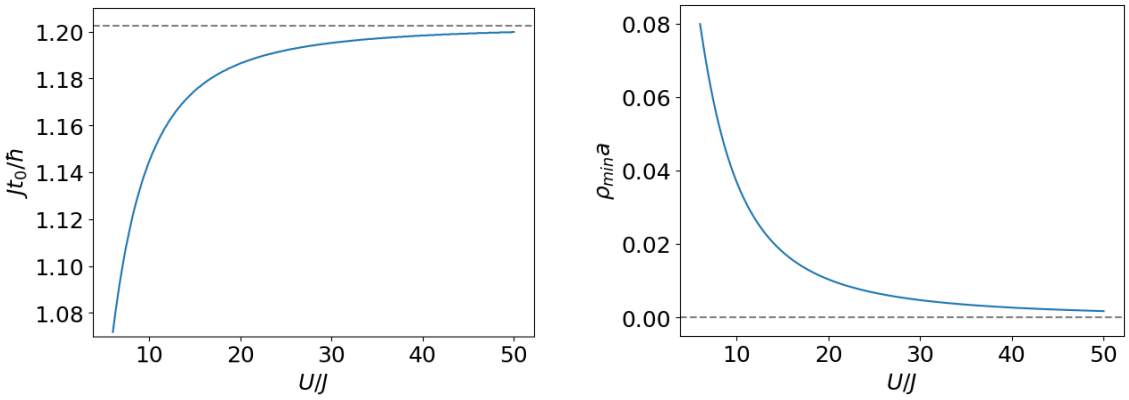

(a) (b)

Figure 5: **(a)** Position of the first minimum of the density over time as a function of U/J. Dashed line represents this position for the Bessel function $J_0(2Jt/\hbar)^2$, the single particle case. **(b)** Height of the first minimum in the density over time as a function of U/J. For $U \to \infty$, $\rho_0(t)$ tends to $J_0(2Jt/\hbar)^2$, which vanishes at every minimum. Dashed line corresponds to the single particle case, where $\rho_0(t_0) = J_0^2(2Jt/\hbar)$.

Since $\rho_0(t)$ is an oscillating function and entails a set of frequencies, we find it interesting to perform the Fourier transform $\mathcal{F}[\rho_0(t)]$ to analyze the frequency spectrum for each value of J/U. Moreover, we associate a single frequency to each plot taking the mean frequency value $\omega^* = \sqrt{\langle\omega^2\rangle}$ (see Fig. 6). The expression used to obtain the mean frequency is

$$\langle\omega^2\rangle = \int_{-\infty}^{\infty} \mathcal{F}(\rho_0(t))\omega^2 d\omega = \int_{-\infty}^{\infty} \hat{\rho}_0(\omega)\omega^2 d\omega. \tag{22}$$

For the single particle case, the Fourier transform of the squared Bessel function can be analytically computed. The result reads

$$\mathcal{F}\left[J_0^2\left(\frac{2Jt}{\hbar}\right)\right] = \frac{K\left(1-\frac{\omega^2}{16}\right)\Pi\left(\frac{\omega}{8}\right)}{\sqrt{2}\pi^{3/2}}, \tag{23}$$

where K is the complete elliptic integral of the first kind (Eq. 24), and $\Pi\left(\frac{\omega}{8}\right)$ is the box function, which vanishes for all $|\omega| > 4$ and gets the value of 1 otherwise.

$$K(m) = \int_0^{\pi/2} \left[1 - m\sin^2(t)\right]^{-1/2} dt. \tag{24}$$

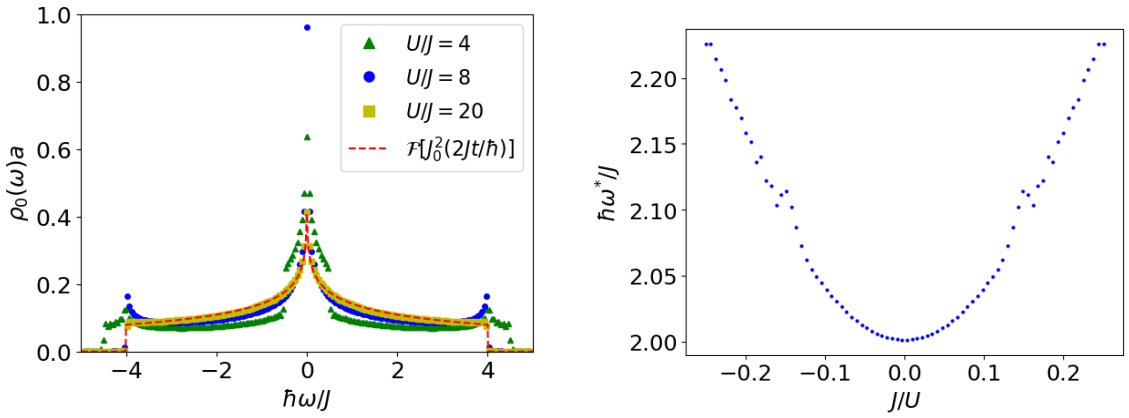

(a) (b)

Figure 6: **(a)** Fourier transform of the density of the central site over time as a function of $\hbar\omega/J$ compared with that of the single particle case (Eq. 23). The sign change of U does not make any difference in the oscillations, hence, the Fourier transforms for positive and negative U are the same. When the interaction strength $|U|$ is increased, the frequency distributions tend to the single particle case, $\mathcal{F}\left[J_0^2\left(2Jt/\hbar\right)\right]$. When U is between the two critical values at which the mass of the hole becomes infinite for $q = 0$ and $q = \pi$ ($|U| < 8$), the frequencies distribution reaches values of $|\hbar\omega/J| > 4$. Additionally, for these values of U, the distributions present a discontinuity whose position approaches to $\hbar\omega/J = 0$ as $|U| \to 8$. When $|U| > 8$, frequencies $|\hbar\omega/J| > 4$ vanish, which also happens in the analytical expression of the single particle case due to the box function. Moreover, the peaks at the maximum frequency decrease as $U \to \infty$. **(b)** Mean frequency of the density in the central site as a function of J/U. For values of $|J/U| > 1/8 = 0.125$, the mean frequencies become less smooth because the maximum frequencies of the spectrum are non-fixed. When $|J/U| < 0.125$, the frequencies are enclosed by the box function.

The dynamics of the system with an initial state with a fully localized hole are not dependent on the sign of the interaction U. No matter if the bosons are repulsive or attractive, the hole density in the initial site over time oscillates in both cases in the same way. This oscillation tends to that of the single particle case when the interaction strength goes to infinity. Hence, increasing the on-site interaction U translates into being able to treat a fully localized hole as a free fully localized boson.

4.1.3 Gaussian space-distributed hole

We analyze the dynamics of a single hole localized in the lattice with a Gaussian distribution. Since this state is not fully localized, it can be defined with a quasimomentum distribution centered at any value q_0,

$$|\psi\rangle = \frac{1}{\sqrt{N}} \sum_{j}^{N_s} e^{-iq_0 j} e^{-\frac{(j-x_0)^2}{2\sigma^2}} |j\rangle\,, \tag{25}$$

where we are using the notation introduced in Eq. 9 and $N = \sum_{j=1}^{N_s} e^{-\frac{(j-x_0)^2}{\sigma^2}}$ is the normalization factor that ensures the normalization of the wave function to unity $\langle\psi|\psi\rangle = 1$.

To capture information about the effective mass of the hole, we compute now the time evolution of the width of the Gaussian distribution and compare it with that of the single particle case, which reads [Dar27]

$$\sigma_{\mathrm{sp}}(t) = \sqrt{\sigma_0^2 + \left(\frac{\hbar t}{m^* \sigma_0}\right)^2}, \tag{26}$$

where σ_0 is the initial width of the distribution and m^* is the effective mass of a single particle in a lattice.

Note that in the single particle case, the value that the effective mass takes is $m^* = 1/(2J)$, obtained from the factor of the second power in q of the expansion of the cosine dispersion relation of Eq. 2. We show how the width of the Gaussian-distributed hole tends to that of the single particle when $U \to \infty$ in Fig. 7,

$$\lim_{U\to\infty} \sigma(J, U, t) = \sigma_{\mathrm{sp}}(J, t) = \sqrt{\sigma_0^2 + \left(\frac{2\hbar t J}{\sigma_0}\right)^2}. \tag{27}$$

To compute the width at every time, we sum the square of all coefficients of the exponential distribution weighed with the square of the distance between the hole and the central point. For $t = 0$, it reads

$$\langle \hat{r}^2 \rangle = \sum_{j=1}^{N_s} \frac{1}{\sqrt{N}} e^{-\frac{(j-x_0)^2}{2\sigma^2}} e^{iq_0 j} (j - x_0)^2 \frac{1}{\sqrt{N}} e^{-iq_0 j} e^{-\frac{(j-x_0)^2}{2\sigma^2}}. \tag{28}$$

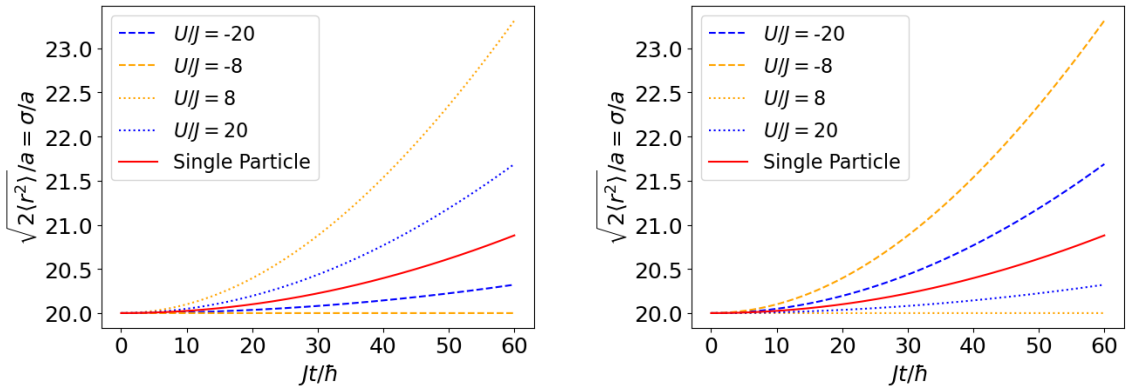

Figure 7: **(a)** Width $\sigma(t)$ of the Gaussian space distribution for the hole with quasimomentum centered at $q = 0$ as a function of time for different values of the interaction strength U. For $U = -8$, the effective mass of the hole is infinity, which is reflected in the constant width of the wave function. **(b)** Width $\sigma(t)$ of the Gaussian space distribution for the hole with quasimomentum centered at $q = \pi$ asa function of time for different values of the interaction strength U. In this case, the effective mass diverges for $U = 8$. Both cases have been computed with an initial width of $\sigma_0 = 10$ and for a lattice which is long enough such that the expansion is not interfering with itself ($N_s = 200$).

Assuming the time evolution of the width of the Gaussian distribution has the same dependence as that of the single particle (Eq. 26), we perfom a fitting with the equation to compute the effective mass as a function of J/U.

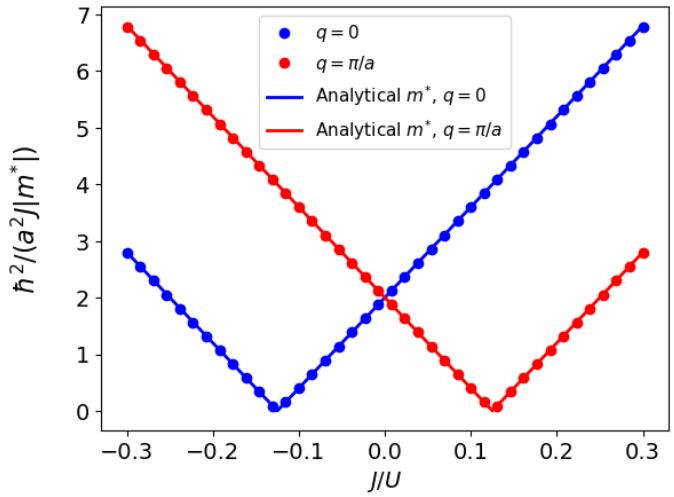

Figure 8: Inverse of the effective mass m^* for a hole with quasimomentum $q = 0$ and $q = \pi$ as a function of J/U. For values $J/U = \pm 1/8 = \pm 0.125$ the inverse mass vanishes, which means that the effective mass tends to infinity, precisely as Eq. 18 suggests analytically.

One can see a perfect agreement between the value of the effective mass obtained from the time evolution of the width of the Gaussian distribution and the analytical expression. This result indicates that the expansion of a Gaussian space distributed hole follows the same dependence as the single particle case (see Eq. 26), even when a superexchange process is present in the Hamiltonian. Moreover, we prove that in the limit $U \to \infty$, the effective mass takes the value of the single particle case, $m^* = 1/(2J)$.

4.1.4 Difference between fully localized and Gaussian distributed holes

We have seen that while the sign modification of U does not produce any difference in the time evolution of the fully localized hole state, it does in the Gaussian distributed state. The reason for this is that the fully localized state has the same overlap value with all eigenstates of the effective Hamiltonian. However, a Gaussian distributed state with quasimomentum $q = 0$ overlaps more with those eigenstates with the lowest energy. In the same way, a Gaussian distributed state with quasimomentum $q = \pi$ overlaps the most with the most excited states (see Fig. 9). Since a sign modification of U yields a shift of π in quasimomentum, a state with a flat quasimomentum ditribution *i.e. fully localized state* is not able to capture any difference when $U \to -U$.

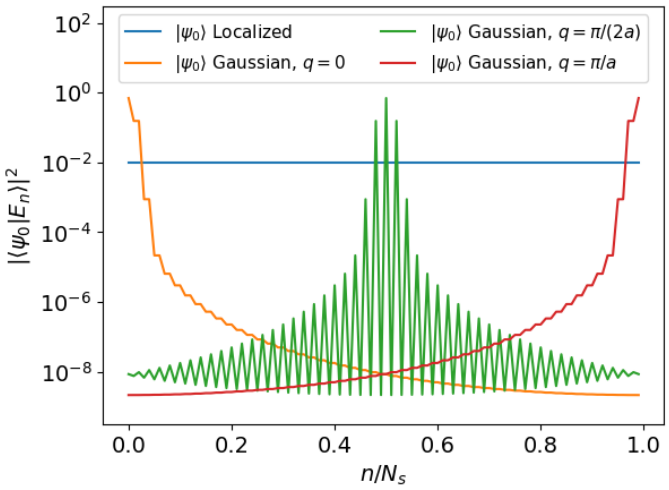

Figure 9: Overlaps of the Gaussian distributed states with three different values of q and the fully localized state with every eigenstate of the effective Hamiltonian. The Gaussian distribution with $q = 0$ overlaps the most with the lowest energy eigenstates, that with $q = \pi$, with the highest, and that with $q = \pi/2$, with those in the middle of the spectrum. The overlap of the localized state is constant, the same for all eigenstates of H_{eff}, and takes the value of $1/N_s$ (this case has been computed for $N_s = 100$).

4.2 Full Hamiltonian

4.2.1 Hole effective mass

In this section we extract the effective mass of the hole using the full Bose-Hubbard Hamiltonian. We obtain the lowest an highest energy bands (for $U > 0$ and $U < 0$ respectively) and associate a certain quasimomentum to each eigenstate. To do so, we introduce the total momentum operator $\hat{Q}$ in momentum space and transform it into real space through the Fourier transform, reading

$$\hat{Q} = \sum_q q\hat{b}_q^\dagger \hat{b}_q = \frac{1}{Ns}\sum_{i,j}\sum_q q e^{iq(j-i)}\hat{b}_j^\dagger \hat{b}_i. \tag{29}$$

After diagonalizing this operator and building the change-of-basis matrix M (eigenvectors of $\hat{Q}$ in columns), we write the Hamiltonian in the momentum basis, $\hat{H}_Q = M^\dagger \hat{H} M$. In this form, the Hamiltonian becomes a block diagonal matrix where each submatrix has a well-defined quasimomentum (shifted to the first Brillouin zone). Hence, diagonalizing each block gives the energy and quasimomentum distribution, this is, the dispersion relation. Note that to check the agreement of this dispersion relation with that of the effective Hamiltonian for any value of U, both positive and negative, we have to look at the lowest band for $U > 0$, and the highest band for $U < 0$.

We compute the effective mass of the hole by calculating the second derivative of the band at a certain q using the method of finite differences at $q = 0$ and $q = \pi$. The expressions read

$$\left.\frac{1}{m^*}\right|_{q=0} = \frac{E(Q=\frac{2\pi}{N_s}) - 2E(Q=0) + E(Q=\frac{-2\pi}{N_s})}{\left(\frac{2\pi}{N_s}\right)^2},$$
$$\left.\frac{1}{m^*}\right|_{q=-\pi} = \frac{E(Q=-\pi\frac{N_s-2}{N_s}) - 2E(Q=-\pi) + E(Q=\pi\frac{N_s-2}{N_s})}{\left(\frac{2\pi}{N_s}\right)^2}, \tag{30}$$

where all quasimomentum values are shifted to the first Brillouin zone. Note that this expression is not valid at $q = 0$ when the first derivative is not continuous. Hence, since a vanishing on-site interaction strength leads to a linear dispersion relation (see Fig. 10), $E(q) = c|q|$, the second derivative computed with finite differences is not valid in this limit.

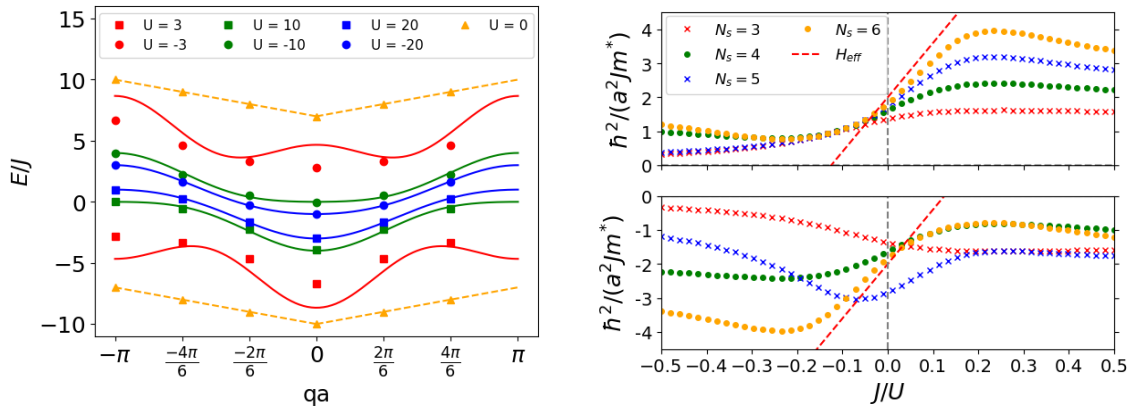

(a) (b)

Figure 10: **(a)** Comparison of energy bands of the full Bose-Hubbard Hamiltonian (squares and circles) with those from the effective Hamiltonian (solid lines) for different values of the on-site interaction energy U. For $U = 0$, yellow dashed line is the analytical fitting for the band described by the full Hamiltonian, it has a linear dependence. **(b)** Inverse effective mass computed with finite differences in the lowest and highest bands of the spectrum for $U > 0$ and $U < 0$ respectively. Upper panel corresponds to this computation at $q = 0$, lower panel corresponds to $q = \pi$. Each panel has the straight line corresponding to the inverse effective mass calculated obtained for the effective Hamiltonian (Eq. 18). For the case $q = \pi$, the results for N_s odd do not agree with the effective Hamiltonian prediction because quasimomentum $q = \pi$ is not existing for those N_s values. Additionally, it is seen that the symmetry $U \to -U$ yielding a shift of π in quasimomentum, is just present for N_s even. Note that the computation of the inverse effective mass with the full Bose-Hubbard Hamiltonian is just valid at $J/U \approx 0$ due the limitation in the finite differences method.

We show that the energy bands obtained from the effective Hamiltonian agree with those from the full Bose-Hubbard Hamiltonian when the interaction strength U is large. Moreover, this result provides an accurate computation of the effective mass of a hole in the same limit. Outside this limit, our result is not valid in the Bose-Hubbard Hamiltonian due to the restriction in the perturbation theory approach. Furthermore, the computation of the effective mass in the full Hamiltonian in a small-sized system with a small interaction strength is not accurate due to the limitation in the calculation of numerical derivatives through finite differences.

4.2.2 Fully localized hole

To compare how accurate our results with the effective Hamiltonian are, we use now the full Bose-Hubbard Hamiltonian to evolve in time an initially fully localized hole and calculate the expectation value of the hole density in the site where the hole was initially located (as we do in Sec. 4.1.2 with the effective Hamiltonian). Note that, since now we are using the full Hamiltonian, there are states with more than one boson per site which were not allowed in the effective Hamiltonian. Notice that working with the full Hamiltonian imposes a limitation on the number of sites due to the size of the Hilbert space.

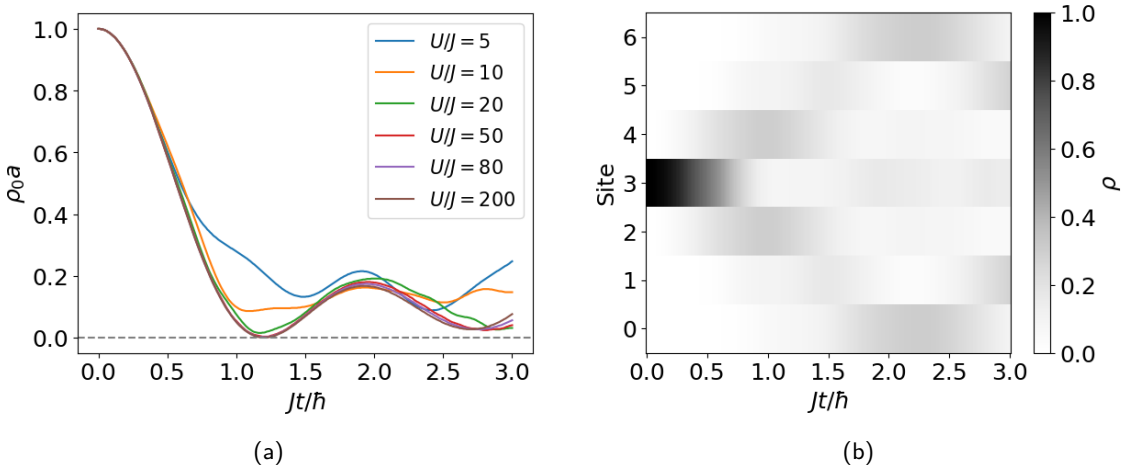

Figure 11: **(a)** Time evolution of density in central site using the full Bose-Hubbard Hamiltonian. For $U \to \infty$ the function tends to the Bessel function $J_0^2(2Jt/\hbar)$. For smaller values of U the function is not analytical. **(b)** Hole density evolution over time and lattice site computed with the full Bose-Hubbard Hamiltonian with $U = 10$. At $Jt/\hbar \approx 2.25$ the hole wavefront reaches the lattice edge, which indicates that its speed over the lattice is $v \approx 1.33\ \hbar/(Jt)$ for $U = 10$.

Our results in the study of the local time evolution of hole density with the full Bose-Hubbard Hamiltonian show remarkable features similar to those observed with the effective Hamiltonian. A constructive interference of the hole wave function produces an oscillating local density over time which vanishes at infinite time, when the hole has fully scattered all over the lattice. Additionally, we have shown that the speed of the hole in the effective Hamiltonian ($v_{\text{eff}} \approx 1.66$) is larger than that obtained from the full Hamiltonian ($v = 1.33$), differing by a 25%. Thus, we have shown that the effective Hamiltonian is a good approximation and that perturbation theory is a valid approach to capture effects present in the full Bose-Hubbard Hamiltonian.

5 Conclusions and Outlook

In this work we have studied the properties of a single-hole system described by the Bose-Hubbard model. We have analyzed the different regimes of the Hamiltonian: non-interacting, Tonks-Girardeau ($U \to \infty$) and strongly interacting regimes. The first two cases can be solved analytically and give rise to a bosonic plane waves spectrum and a Fermi sea spectrum, respectively. The third limit requires both numerical methods such as exact diagonalization (ED) and the approximation analytical tool of perturbation theory.

We have performed degenerate perturbation theory method and obtained an effective Hamiltonian both in matrix and operator forms. In the latter form, we have introduced

the concept of "hole" as a quasi-particle and defined its creation and annihilation operators in second quantization. The operator formalism has allowed us to analytically solve the effective Hamiltonian, leading us to the hole dispersion relation, which relates the quasimomentum of a hole and its energy. At $q = 0$ and $q = \pi$, the hole dispersion relation presents either a maximum or a minimum, which indicates a vanishing linear q dependence for certain values of J/U. Hence, we have investigated the effective mass of the hole at these quasimomentum values. The value of the effective mass is not reflected in the time evolution of a state with a fully localized hole due to the constant distribution of the overlaps with the eigenstates of the effective Hamiltonian. However, the effective mass can be obtained from the time evolution of a space Gaussian distributed hole by analyzing the time dependence of the width of the distribution. In both the localized and Gaussian distributed hole, a single particle behavior is observed in the limit of infinite on-site interaction, both attractive and repulsive.

To finalize, we have compared our previous results obtained with the effective Hamiltonian with those obtained from the Bose-Hubbard Hamiltonian. The computation of the effective mass has been restricted by the limitation in the limits of validity of out numerical methods. For that reason, our results for the effective mass computed with the Bose-Hubbard Hamiltonian are valid in the limit $J/|U| \lesssim 0.1$, where they agree with those from the effective Hamiltonian.

As an extension of this work, it would be interesting to compute the effective mass in the full Bose-Hubbard model for any interaction strength U. To do so, we would need to numerically compute the second derivative for functions that are not smooth, such as the dispersion relation $E = c|q|$. Moreover, a study of the system with two holes or more could bring new features. Finally, a better understanding of the dynamics of such systems could be achieved by adding long-range interactions between atoms, such as dipolar interactions.

Bibliography

[ABB+18] Antonio Acín, Immanuel Bloch, Harry Buhrman, Tommaso Calarco, Christopher Eichler, Jens Eisert, Daniel Esteve, Nicolas Gisin, Steffen J Glaser, Fedor Jelezko, Stefan Kuhr, Maciej Lewenstein, Max F Riedel, Piet O Schmidt, Rob Thew, Andreas Wallraff, Ian Walmsley, and Frank K Wilhelm. The quantum technologies roadmap: a european community view. *New Journal of Physics*, 20(8):080201, 2018.

[AEM+95] M. H. Anderson, J. R. Ensher, M. R. Matthews, C. E. Wieman, and E. A. Cornell. Observation of bose-einstein condensation in a dilute atomic vapor. *Science*, 269(5221):198–201, 1995.

[AKL+17] Grigory E. Astrakharchik, Konstantin V. Krutitsky, Maciej Lewenstein, Ferran Mazzanti, and Jordi Boronat. Optical lattices as a tool to study defect-induced superfluidity. *Phys. Rev. A*, 96(3), 2017.

[Ast14] G. Astrakharchik. Quantum monte carlo study of ultracold gases. PhD thesis, 2014.

[BCMS19] Colin D. Bruzewicz, John Chiaverini, Robert McConnell, and Jeremy M. Sage. Trapped-ion quantum computing: Progress and challenges. *Applied Physics Reviews*, 6(2):021314, 2019.

[BCS57] J. Bardeen, L. N. Cooper, and J. R. Schrieffer. Theory of superconductivity. *Phys. Rev.*, 108:1175–1204, 1957.

[BDG22] Annabelle Bohrdt, Eugene Demler, and Fabian Grusdt. Dichotomy of heavy and light pairs of holes in the $t-j$ model. arXiv: 2210.02322, 2022.

[BHB+22] Annabelle Bohrdt, Lukas Homeier, Immanuel Bloch, Eugene Demler, and Fabian Grusdt. Strong pairing in mixed-dimensional bilayer antiferromagnetic mott insulators. *Nature Physics*, 18(6):651–656, 2022.

[BHR+21] Annabelle Bohrdt, Lukas Homeier, Christian Reinmoser, Eugene Demler, and Fabian Grusdt. Exploration of doped quantum magnets with ultracold atoms. *Annals of Physics*, 435:168651, 2021.

[BSH97] C. C. Bradley, C. A. Sackett, and R. G. Hulet. Bose-einstein condensation of lithium: Observation of limited condensate number. *Phys. Rev. Lett.*, 78:985–989, 1997.

[BSTH95] C. C. Bradley, C. A. Sackett, J. J. Tollett, and R. G. Hulet. Evidence of bose-einstein condensation in an atomic gas with attractive interactions. *Phys. Rev. Lett.*, 75:1687–1690, 1995.

[Caz03] M. A. Cazalilla. One-dimensional optical lattices and impenetrable bosons. *Phys. Rev. A*, 67(5), 2003.

[CLRS11] François Crépin, Nicolas Laflorencie, Guillaume Roux, and Pascal Simon. Phase diagram of hard-core bosons on clean and disordered two-leg ladders: Mott insulator–luttinger liquid–bose glass. *Phys. Rev. B*, 84:054517, 2011.

[CSPS07] B. Capogrosso-Sansone, N. V. Prokof'ev, and B. V. Svistunov. Phase diagram and thermodynamics of the three-dimensional bose-hubbard model. *Phys. Rev. B*, 75:134302, 2007.

[CSSPS08] B. Capogrosso-Sansone, Şebnem Güne ş Söyler, Nikolay Prokof'ev, and Boris Svistunov. Monte carlo study of the two-dimensional bose-hubbard model. *Phys. Rev. A*, 77:015602, 2008.

[Dar27] Charles Galton Darwin. Free motion in the wave mechanics. *Proceedings of the Royal Society of London. Series A, Containing Papers of a Mathematical and Physical Character*, 117(776):258–293, 1927.

[DMA+95] K. B. Davis, M. O. Mewes, M. R. Andrews, N. J. van Druten, D. S. Durfee, D. M. Kurn, and W. Ketterle. Bose-einstein condensation in a gas of sodium atoms. *Phys. Rev. Lett.*, 75:3969–3973, 1995.

[DWM04] M. H. Devoret, A. Wallraff, and J. M. Martinis. Superconducting qubits: A short review. arXiv:cond-mat/0411174, 2004.

[FCM+11] Shiang Fang, Chia-Min Chung, Ping Nang Ma, Pochung Chen, and Daw-Wei Wang. Quantum criticality from in situ density imaging. *Phys. Rev. A*, 83:031605, 2011.

[FK07] Liang Fu and C. L. Kane. Topological insulators with inversion symmetry. *Phys. Rev. B*, 76(4), 2007.

[FKW+98] Dale G. Fried, Thomas C. Killian, Lorenz Willmann, David Landhuis, Stephen C. Moss, Daniel Kleppner, and Thomas J. Greytak. Bose-einstein condensation of atomic hydrogen. *Phys. Rev. Lett.*, 81:3811–3814, 1998.

[GME+02] Markus Greiner, Olaf Mandel, Tilman Esslinger, Theodor W Hänsch, and Immanuel Bloch. Quantum phase transition from a superfluid to a mott insulator in a gas of ultracold atoms. *Nature*, 415(6867):39–44, 2002.

[HCB+23] Sarah Hirthe, Thomas Chalopin, Dominik Bourgund, Petar Bojović, Annabelle Bohrdt, Eugene Demler, Fabian Grusdt, Immanuel Bloch, and Timon A. Hilker. Magnetically mediated hole pairing in fermionic ladders of ultracold atoms. *Nature*, 613(7944):463–467, 2023.

[HJG+98] R.J Hughes, D.F.V. James, J.J. Gomez, M.S. Gulley, M.H. Holzscheiter, P.G. Kwiat, S.K. Lamoreaux, C.G. Peterson, V.D. Sandberg, M.M. Schauer, C.M. Simmons, C.E. Thorburn, D. Tupa, P.Z. Wang, and A.G. White. The los alamos trapped ion quantum computer experiment. *Fortschritte der Physik*, 46(4-5):329–361, 1998.

[HWFZ20] He-Liang Huang, Dachao Wu, Daojin Fan, and Xiaobo Zhu. Superconducting quantum computing: a review. *Science China Information Sciences*, 63(8), 2020.

[JBC+98] D. Jaksch, C. Bruder, J. I. Cirac, C. W. Gardiner, and P. Zoller. Cold bosonic atoms in optical lattices. *Phys. Rev. Lett.*., 81(15):3108–3111, 1998.

[JW28] Pascual Jordan and Eugene P. Wigner. About the Pauli exclusion principle. *Z. Phys.*, 47:631–651, 1928.

[Kap03] P. Kapitza. *1938. Viscosity of liquid helium below the -point*, pages 58–60. University of Chicago Press, Chicago, 2003.

[Koh64] Walter Kohn. Theory of the insulating state. *Phys. Rev.*, 133:A171–A181, 1964.

[Kru16] Konstantin V. Krutitsky. Ultracold bosons with short-range interaction in regular optical lattices. *Physics Reports*, 607:1–101, 2016.

[KWM00] Till D. Kühner, Steven R. White, and H. Monien. One-dimensional bose-hubbard model with nearest-neighbor interaction. *Phys. Rev. B*, 61(18):12474–12489, 2000.

[Leg99] A. J. Leggett. Superfluidity. *Rev. Mod. Phys.*, 71:S318–S323, 1999.

[LGSV98] E Louis, F Guinea, M. P. Ló pez Sancho, and J. A Vergés. Hole pairs in the two-dimensional hubbard model. *Europhysics Letters (EPL)*, 44(2):229–234, 1998.

[LSA+07] Maciej Lewenstein, Anna Sanpera, Veronica Ahufinger, Bogdan Damski, Aditi Sen(De), and Ujjwal Sen. Ultracold atomic gases in optical lattices: mimicking condensed matter physics and beyond. *Advances in Physics*, 56(2):243–379, 2007.

[LZ09] Jon Links and Shao-You Zhao. A bethe ansatz study of the ground state energy for the repulsive bose–hubbard dimer. *Journal of Statistical Mechanics: Theory and Experiment*, 2009(03):P03013, 2009.

[MBHD21] Ivan Morera, Annabelle Bohrdt, Wen Wei Ho, and Eugene Demler. Attraction from frustration in ladder systems. arXiv:2106.09600, 2021.

[MCJ+17] Anton Mazurenko, Christie S. Chiu, Geoffrey Ji, Maxwell F. Parsons, Márton Kanász-Nagy, Richard Schmidt, Fabian Grusdt, Eugene Demler, Daniel Greif, and Markus Greiner. A cold-atom fermi–hubbard antiferromagnet. *Nature*, 545(7655):462–466, 2017.

[MDK+11] K. W. Mahmud, E. N. Duchon, Y. Kato, N. Kawashima, R. T. Scalettar, and N. Trivedi. Finite-temperature study of bosons in a two-dimensional optical lattice. *Phys. Rev. B*, 84(5), 2011.

[Mis12] Prasanta K. Misra. Physics of condensed matter. Academic Press, Boston, 2012.

[MKNS+23] Ivan Morera, Márton Kanász-Nagy, Tomasz Smolenski, Livio Ciorciaro, Ata ç Imamoğlu, and Eugene Demler. High-temperature kinetic magnetism in triangular lattices. *Phys. Rev. Res.*, 5:L022048, 2023.

[Mor22] Ivan Morera. Exotic phases of matter in low dimensional lattices: from quantum liquids to kinetic magnetism. Phd thesis, 2022.

[RB03] R. Roth and K. Burnett. Superfluidity and interference pattern of ultracold bosons in optical lattices. *Phys. Rev. A*, 67:031602, 2003.

[RGLJD17] David Raventó s, Tobias Graß, Maciej Lewenstein, and Bruno Juliá-Díaz. Cold bosons in optical lattices: a tutorial for exact diagonalization. *Journal of Physics B: Atomic, Molecular and Optical Physics*, 50(11):113001, 2017.

[Sch11] Ulrich Schollwöck. The density-matrix renormalization group in the age of matrix product states. *Annals of Physics*, 326(1):96–192, 2011.

[SFS+20] Florian Schäfer, Takeshi Fukuhara, Seiji Sugawa, Yosuke Takasu, and Yoshiro Takahashi. Tools for quantum simulation with ultracold atoms in optical lattices. *Nature Reviews Physics*, 2(8):411–425, 2020.

[SSBG23] Henning Schlömer, Ulrich Schollwöck, Annabelle Bohrdt, and Fabian Grusdt. Kinetic-to-magnetic frustration crossover and linear confinement in the doped triangular $t - j$ model. arXiv:2305.02342, 2023.

[WF04] Steven R. White and Adrian E. Feiguin. Real-time evolution using the density matrix renormalization group. *Phys. Rev. Lett.*, 93:076401, 2004.

[Whi92] Steven R. White. Density matrix formulation for quantum renormalization groups. *Phys. Rev. Lett.*, 69:2863–2866, 1992.

[Whi93] Steven R. White. Density-matrix algorithms for quantum renormalization groups. *Phys. Rev. B*, 48:10345–10356, 1993.

[WHR15] M. L. Wall, K. R. A. Hazzard, and A. M. Rey. Quantum magnetism with ultracold molecules. In *From Atomic to Mesoscale*, pages 3–37. WORLD SCIENTIFIC, 2015.

[WK22] Tom Westerhout and Mikhail I. Katsnelson. Role of correlated hopping in the many-body physics of flat-band systems: Nagaoka ferromagnetism. *Phys. Rev. B*, 106(4), 2022.

[ZD10] J M Zhang and R X Dong. Exact diagonalization: the bose–hubbard model as an example. *European Journal of Physics*, 31(3):591–602, 2010.

[ZKKT09] Qi Zhou, Yasuyuki Kato, Naoki Kawashima, and Nandini Trivedi. Direct mapping of the finite temperature phase diagram of strongly correlated quantum models. *Phys. Rev. Lett.*, 103:085701, 2009.

[Zwi14] Martin W. Zwierlein. Superfluidity in ultracold atomic Fermi gases. In *Novel Superfluids: Volume 2*. Oxford University Press, 2014.

Appendices

A Python code

A.1 Fock basis creation

Here we attach the Python code used to create the basis of Fock states. We have written the code for the case of two different species. To be used with a single species, just set $N_b = 0$.

```
def tuple_sum(a,b):
    output = ()
    for i in range(len(a)):
        output += ((a[i]+b[i]),)
    return output

def create_next_set(set_ini):
    v = set_ini.pop()
    set_ini.add(v)
    N = len(v)
    idty = np.eye(N,dtype=int)
    output = set()
    for i in set_ini:
        for j in idty:
            j = tuple(j)
            output.add(tuple_sum(i,j))
    return output

def create_whole_set(N,Ns):
    ini_vec = tuple((0 for _ in range (Ns)))
    ini_set = set()
    ini_set.add(ini_vec)
    for _ in range(N):
        #print(ini_set)
        ini_set = create_next_set(ini_set)
    return ini_set

def create_whole_basis(Na,Nb,Ns):
    set_a = create_whole_set(Na,Ns)
    set_b = create_whole_set(Nb,Ns)
    basis = []

    for i in (set_a):
        for j in (set_b):
            #current_vector = np.array((Ns,2))
            current_vector = []
            for k in range(Ns):
                secondary_vector = [i[k],j[k]]
                current_vector.append(secondary_vector)
            current_vector = np.array(current_vector)
```

```
            basis.append(current_vector)

    return basis
```

A.2 Construction of Hamiltonian

Here we attach the Python code to create the operators that define the Bose-Hubbard Hamiltonian. Every operator is defined as a function that receives a Fock state as input, and gives as output a new Fock state and a factor. The construction of the Hamiltonian requires the basis, which is obtained in Appendix A.1.

```
def c(ket,i,species):
    outket = ket.copy()
    if ket[i,species] > 0:
        outfactor = math.sqrt(outket[i,species])
        outket[i,species] = outket[i,species] -1
    elif ket[i,species] <= 0:
        outfactor = 0
        outket[i,species] = 0
    return outfactor,outket

def c_dagger(ket,i,species):
    outket = ket.copy()
    if (i>(len(ket)-1)):
        outfactor = 0
        #outket[i,species] = outket[i,species]
    else:
        outfactor = math.sqrt(outket[i,species]+ 1)
        outket[i,species] = outket[i,species] + 1
    return outfactor,outket

def hopping_right(i,species,ket):
    outket = ket.copy()
    if (i == len(ket)-1):
        factor1 = 0
        factor2 = 0
    elif (i<(len(ket)-1)):
        factor1, outket = c(outket,i,species)
        factor2, outket = c_dagger(outket,i+1,species)
    outfactor = factor1*factor2
    return outfactor, outket

def hopping_left(i,species,ket):
    outket = ket.copy()
    if (i == 0):
        factor1 = 0
        factor2 = 0
    elif (i>0):
        factor1, outket = c(outket,i,species)
        factor2, outket = c_dagger(outket,i-1,species)
```

```
    outfactor = factor1*factor2
    return outfactor, outket

def n(i,species,ket):
    outket = ket.copy()
    factor1, outket = c(outket,i,species)
    factor2, outket = c_dagger(outket,i,species)
    outfactor = factor1*factor2
    return outfactor, outket

def H_hopping_element_single_site(bra,ket,i):
    output = 0

    for alpha in range(2):
        outfactor_l,outket_l = hopping_left(i,alpha,ket)
        outfactor_r,outket_r = hopping_right(i,alpha,ket)
        if np.array_equal(bra,outket_l):
            output = output - outfactor_l
        if np.array_equal(bra,outket_r):
            output = output - outfactor_r
    return output


def total_H_hopping_element(bra,ket):
    output = 0
    for i in range(len(bra)):
        output = output + H_hopping_element_single_site(bra,ket,i)
    return output

def build_H_hopping(basis):
    H = np.zeros((len(basis), len(basis)))
    for i in range(len(basis)):
        for j in range(len(basis)):
            bra = basis[i]
            ket = basis[j]
            H[i,j] = total_H_hopping_element(bra,ket)
    return H


def H_contact_element_single_site(bra,ket,i):
    output = 0

    for alpha in range(2):
        outfactor_c, outket_c = n(i,alpha,ket)
        if np.array_equal(bra,outket_c):
            output = output + outfactor_c*(outfactor_c-1)*1/2
    return output
```

```
def total_H_contact_element(bra,ket):
    output = 0
    for i in range(len(bra)):
        output = output + H_contact_element_single_site(bra,ket,i)
    return output

def build_H_contact(basis):
    H = np.zeros((len(basis),len(basis)))
    for i in range(len(basis)):
        for j in range(len(basis)):
            bra = basis[i]
            ket = basis[j]
            H[i,j] = total_H_contact_element(bra,ket)
    return H
```

B $\hat{H}_J$ in momentum space

The kinetic term of the bose-Hubbard Hamiltonian can be written in momentum space. To do so, one needs to apply a Fourier transform on the creation and annihilation operators. The new operators obtained after the transformation, $\hat{b}_q^\dagger$, $\hat{b}_q$, create and annihilate a boson with a certain quasimomentum q instead of defining their position. The transformation reads as

$$\begin{aligned} \hat{b}_j^\dagger &= \frac{1}{\sqrt{N_s}} \sum_q e^{-iqx_j} \hat{b}_q^\dagger, \\ \hat{b}_j &= \frac{1}{\sqrt{N_s}} \sum_q e^{iqx_j} \hat{b}_q, \end{aligned} \tag{31}$$

where the lattice spacing is set to unit and hence, $x_j \equiv j$. Substituting the operators $\hat{b}_i$ and $\hat{b}_i^\dagger$ for $\hat{b}_q$ and $\hat{b}_q^\dagger$ respectively, we obtain the new Hamiltonian

$$\hat{H}_J = -J \sum_{qq'} \left[e^{-iq} \sum_j \frac{1}{N_s} e^{-i(q-q')j} \hat{b}_q^\dagger \hat{b}_{q'} + \text{h.c.} \right]. \tag{32}$$

Imposing that the exponentials form an orthonormal and complete basis, the sum over j equals $N_s \delta_{q,q'}$, which yields to a much more simple expression,

$$\hat{H}_J = -J \sum_q \left[e^{-iq} \hat{n}_q + \text{h.c.} \right] = -2J \sum_q \hat{n}_q \cos q. \tag{33}$$

C Fermi sea energy

The ground state of a non-interacting fermionic system described by a hopping Hamiltonian can be obtained by computing the sum over the lowest quasimomentum occupied states (see Eq. 33 from Appendix B), which reads

$$E_0 = -2J \sum_q \cos q. \tag{34}$$

The quasimomentum q in a fermionic system takes values $2\pi k/N_s$, where $k \in [-k_{\max}/2, k_{\max}/2]$. Hence, the ground state reads

$$E_0 = -2J \sum_{k=-k_{max}/2}^{k_{max}/2} \cos\left(\frac{2\pi}{N_s}k\right). \tag{35}$$

The cosine of the sum can be rewritten, using Euler's identity, as

$$\sum_{k=-k_{max}/2}^{k_{max}/2} \cos\left(\frac{2\pi}{N_s}k\right) = \frac{1}{2}\sum_{k=-k_{max}/2}^{k_{max}/2} e^{i\frac{2\pi}{N_s}k} + e^{-i\frac{2\pi}{N_s}k}. \tag{36}$$

Using the change of variables $k' = k + \frac{k_{max}}{2}$, reads

$$\frac{1}{2}\sum_{k'=0}^{k_{max}} \left[e^{i\frac{2\pi}{N_s}k'} e^{-i\pi\frac{k_{max}}{N_s}} + e^{-i\frac{2\pi}{N_s}k'} e^{i\pi\frac{k_{max}}{N_s}}\right]. \tag{37}$$

Since the sum over the occupation number has as many terms as particles in the system, the maximum value of the quasimomentum is defined by $k_{\max} = N-1$. Setting the variable $z = \frac{1}{2}\sum_{k'=0}^{N-1}\left[e^{i\frac{2\pi}{N_s}k}e^{-i\pi\frac{N-1}{N_s}}\right]$, we see that the sum we are looking for is $2\Re(z) = \Re\left(e^{-i\pi\frac{N-1}{N_s}}\sum_{k=0}^{N-1} e^{i\frac{2\pi}{N_s}k}\right)$. To solve the sum we can use the geometric series, which gives

$$\begin{aligned}\sum_{k=0}^{N-1} e^{i\frac{2\pi}{N_s}k} = \frac{1-e^{i\frac{2\pi}{N_s}N}}{1-e^{i\frac{2\pi}{N_s}}} = \frac{1-e^{i\frac{2\pi}{N_s}N}}{e^{i\frac{\pi}{N_s}}\left(e^{-i\frac{\pi}{N_s}} - e^{i\frac{\pi}{N_s}}\right)} = \frac{e^{-i\pi/N_s}}{-2i\sin\pi/N_s}\left(1-e^{i\frac{2\pi}{N_s}N}\right) = \\ \frac{e^{-i\pi/N_s}}{\sin\pi/N_s}\frac{-2i}{-2i}e^{i\pi n}\left(e^{-i\pi n} - e^{i\pi n}\right) = \frac{\sin\pi n}{\sin\frac{\pi}{N_s}}e^{i\frac{\pi}{N_s}(N-1)}.\end{aligned} \tag{38}$$

Hence, since we need the real part of the product of the last result with the exponential $e^{-i\frac{\pi}{N_s}(N-1)}$, we get

$$\Re\left(e^{-i\pi\frac{N-1}{N_s}}\sum_{k=0}^{N-1} e^{i\frac{2\pi}{N_s}k}\right) = \frac{\sin\pi n}{\sin\frac{\pi}{N_s}}. \tag{39}$$

Finally, we add the factor $-2J$ and obtain

$$E_J = -2J\frac{\sin\pi n}{\sin\frac{\pi}{N_s}}. \tag{40}$$

D Degenerate perturbation theory

D.1 Toy example. $N = 2$, $N_s = 3$

Let us study the system with $N = 2$, $N_s = 3$. To obtain corrections up to second order in degenerate perturbation theory we need to diagonalize the effective Hamiltonian, whose matrix elements read

$$\hat{H}_{\text{eff}} = \langle\alpha|\hat{H}_J|\beta\rangle - \frac{1}{2}\sum_{\gamma}\langle\alpha|\hat{H}_J|\gamma\rangle\langle\gamma|\hat{H}_J|\beta\rangle\left(\frac{1}{E_\gamma - E_\alpha} + \frac{1}{E_\gamma - E_\beta}\right) = \hat{H}^{(1)}_{\text{eff}} + \hat{H}^{(2)}_{\text{eff}}. \tag{41}$$

States $|\alpha\rangle, |\beta\rangle$ are the degenerate eigenstates of the unperturbed Hamiltonian $\hat{H}_U$ and $|\gamma\rangle$ is any state that does not belong to the degenerate subspace of $|\alpha\rangle$ and $|\beta\rangle$. Consider

the basis $\{|0\rangle, |1\rangle, |2\rangle, |3\rangle, |4\rangle, |5\rangle\} = \{|1,1,0\rangle, |1,0,1\rangle, |0,1,1\rangle, |2,0,0\rangle, |0,2,0\rangle, |0,0,2\rangle\}$. It can easily be seen that, using the unperturbed Hamiltonian $\hat{H}_U$, the first three elements of the basis share an energy of $E = 0$ and are the ground state of $\hat{H}_U$. Moreover, the last three elements have an energy of $E = U$ and are the excited state of $\hat{H}_U$. There are two energy levels three times degenerate each, it is the ideal situation to use degenerate perturbation theory.

The ground state first order corrections are obtained by diagonalizing the first order effective Hamiltonian in the subspace of degenerate ground states of $\hat{H}_U$, this is, diagonalizing the matrix given by the matrix elements $\langle\alpha|\hat{H}_J|\beta\rangle$, which form the effective Hamiltonian $\hat{H}^{(1)}_{\text{eff}}$. The states $|\alpha\rangle$ and $|\beta\rangle$ are the first three states of the basis. It is straight forward to see that the matrix and its eigenvalues read

$$\hat{H}^{(1)}_{\text{eff}} = \begin{pmatrix} 0 & -J & -J \\ -J & 0 & -J \\ -J & -J & 0 \end{pmatrix} \quad \rightarrow \quad \begin{cases} \lambda_0 = -2J, \\ \lambda_1 = J, \\ \lambda_2 = J. \end{cases} \tag{42}$$

Up to first order, the degeneracy of the first three degenerate states of $\hat{H}_U$ is not completely broken since two states are still degenerate. For the excited states $|3\rangle, |4\rangle, |5\rangle$ the degeneracy is not broken at first order since the perturbation $\hat{H}_J$ cannot connect any of those states ($\hat{H}^{(1)}_{\text{eff}} = 0$).

To get the second order correction of the ground state, we need to obtain the effective Hamiltonian up to second order using both terms of Eq. 41. The matrix and its eigenvalues read

$$\hat{H}^{(1)}_{\text{eff}} + \hat{H}^{(2)}_{\text{eff}} = \begin{pmatrix} 0 & -J & -J \\ -J & 0 & -J \\ -J & -J & 0 \end{pmatrix} + \begin{pmatrix} \frac{-4J^2}{U} & \frac{-2J^2}{U} & \frac{-2J^2}{U} \\ \frac{-2J^2}{U} & \frac{-4J^2}{U} & \frac{-2J^2}{U} \\ \frac{-2J^2}{U} & \frac{-2J^2}{U} & \frac{-4J^2}{U} \end{pmatrix} \quad \rightarrow \quad \begin{cases} \lambda_0 = -2J - \dfrac{8J^2}{U}, \\ \lambda_1 = J - \dfrac{2J^2}{U}, \\ \lambda_2 = J - \dfrac{2J^2}{U}. \end{cases} \tag{43}$$

Degeneracy of the ground state is still not completely broken up to second order corrections. To compute the second order correction for the excited states we need to find the eigenvalues of the matrix given by Eq. 41 in the subspace of the degenerate excited states of $\hat{H}_U$, the states $|\alpha\rangle, |\beta\rangle = |3\rangle, |4\rangle, |5\rangle$ (Note that the first order matrix is zero). The resultant matrix and its eigenvalues read

$$\hat{H}^{(2)}_{\text{eff}} = \begin{pmatrix} \frac{4J^2}{U} & \frac{2J^2}{U} & \frac{2J^2}{U} \\ \frac{2J^2}{U} & \frac{4J^2}{U} & \frac{2J^2}{U} \\ \frac{2J^2}{U} & \frac{2J^2}{U} & \frac{4J^2}{U} \end{pmatrix} \quad \rightarrow \quad \begin{cases} \lambda_0 = \dfrac{2J^2}{U}, \\ \lambda_1 = \dfrac{2J^2}{U}, \\ \lambda_2 = \dfrac{8J^2}{U}. \end{cases} \tag{44}$$

Hence, the degeneracy of the excited is not completely broken.

We can now compare how the degeneracy is broken by taking results from exact diagonalization and those from perturbation theory.

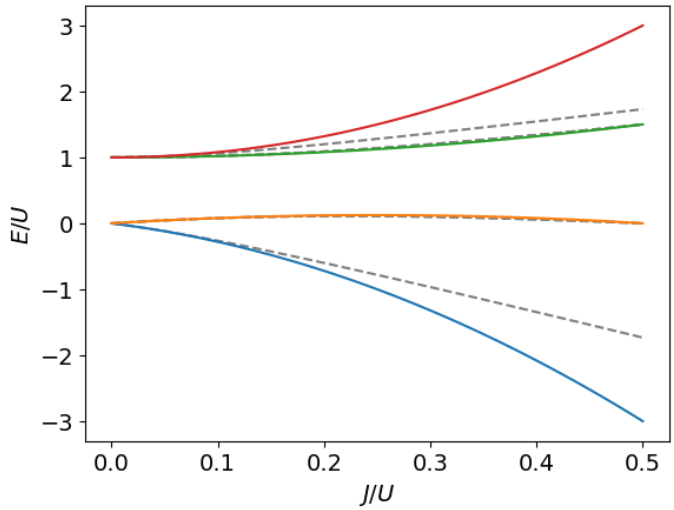

Figure 12: Degeneracy breaking for the system with $N = 2$, $N_s = 3$ and p.b.c. Dashed gray lines correspond to the eigenstates of the full Bose-Hubbard Hamiltonian. Solid coloured lines correspond to the eigenstates of the effective Hamiltonian. Orange and green lines are degenerate. For small values of J/U, perturbation theory works very good and agrees with the full model.

We can check the relative error of perturbation theory in the enrgy of the ground state as a function of the perturbative parameter.

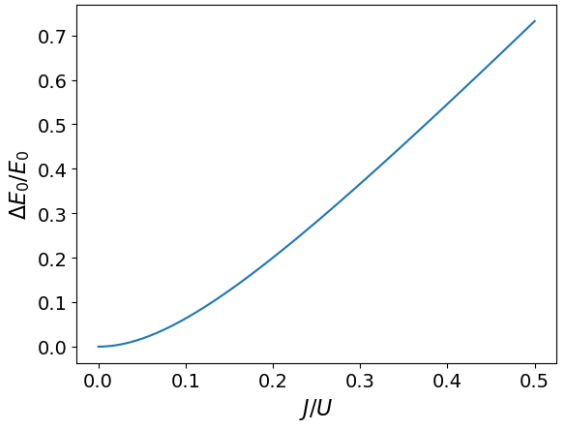

Figure 13: Relative error of the ground state energy of the system as a function of J/U ($\Delta E_0 = |E_0^{\text{eff}} - E_0|$). For an approximate ratio $J/U < 0.1$, the error is less than 10%, which can be considered as a good approximation. Afterwards, this percentage increases linearly with J/U.

D.2 Effective Hamiltonian. Matrix form

To obtain an effective Hamiltonian from the Bose-Hubbard Hamiltonian with $N = N_s - 1$ for the lowest manifold, we need to compute the matrix elements given by Eq. 41. States $|\alpha\rangle$ and $|\beta\rangle$ are all the degenerate eigenstates of $\hat{H}_U$ with the lowest energy, and $|\gamma\rangle$ are all states from the original Hilbert space that do not belong to the subspace of lowest energy of the spectrum of $\hat{H}_U$. Since the lowest manifold can be described by as many states as sites in the lattice, N_s, we use the notation describing the position of the hole in the lattice,

$$|3\rangle = |1, 1, 0, 1, 1, 1..., 1\rangle\,, \quad |5\rangle = |1, 1, 1, 1, 0, 1, 1..., 1\rangle\,. \tag{45}$$

The first order correction in Eq. 41 consists of a single hopping connection of two states which both belong the the lowest energy manifold. Given that the Hamiltonian that connects both states performs a hopping of a boson to first neighbor lattice site, the corresponding matrix elements read

$$\langle n|\, \hat{H}_{\text{eff}}^{(1)}\, |m\rangle = -J(\delta_{n,m-1} + \delta_{n,m+1}). \tag{46}$$

The second order correction consists of both diagonal and non-diagonal terms. Let us obtain first the diagonal ones. Note that the process yielding diagonal terms has to perform a hopping of a boson to an occupied lattice site (due to the constraint of $|\gamma\rangle$ states not to belong to the initial degenerate subspace), and brings it back to the initial site. It is straighforward to see from Eq. 41 that this process results in a factor of $\frac{-2J^2}{U}$. Since we have to sum over all intermediate states $|\gamma\rangle$, we just need to multiply the amount of these states, which is $2(N_s-2)$, by the previous factor. Hence, the diagonal terms read

$$\langle n|\, \hat{H}_{\text{eff}}^{(2)}\, |m\rangle = -2(N_s-2)\frac{2J^2}{U}\delta_{n,m}. \tag{47}$$

The last second order correction is that obtained by connecting two different states of the lowest manifold of $\hat{H}_U$ by means of two hoppings. Following the requirements of Eq 41, the only states $|\beta\rangle$ to which an initial state $|\alpha\rangle$ can be connected are those where the hole is located two sites apart from the initial position. The amplitude of this process is, again, $\frac{-2J^2}{U}$. Thus, the final matrix elements read

$$-\frac{2J^2}{U}(\delta_{n,m-2} + \delta_{n,m+2}). \tag{48}$$

Combining the three terms that we have obtained and taking into account periodic boundary conditions, which translates into $\langle 1|N_s+1\rangle = 1$, $\langle 2|N_s+2\rangle = 1$, the final effective Hamltonian matrix elements can be written as

$$\langle n|\, \hat{H}_{\text{eff}}\, |m\rangle = -J(\delta_{n,m-1} + \delta_{n,m+1}) - 2(N_s-2)\frac{2J^2}{U}\delta_{n,m} - \frac{2J^2}{U}(\delta_{n,m-2} + \delta_{n,m+2}). \tag{49}$$

D.3 Effective Hamiltonian. Hard-core bosons operators

We can write the effective Hamiltonian from Eq. 49 in operator form. Since we restrict the spectrum to that of hard-core bosons, where there is no more than a single boson per site, we can use hard-core bosons operators $\hat{a}_i^\dagger$ and $\hat{a}_i$, which create and annihiliate a hard-core boson at site i respectively. They have mixed commutation and anticommutation relations, $[\hat{a}_i, \hat{a}_j^\dagger] = [\hat{a}_i, \hat{a}_j] = [\hat{a}_i^\dagger, \hat{a}_j^\dagger] = 0$ for $i \neq j$, $\{\hat{a}_i, \hat{a}_i^\dagger\} = 1$ and $(\hat{a}_i)^2 = (\hat{a}_i^\dagger)^2 = 0$ [CLRS11].

Each factor of the effective Hamiltonian is obtained by the perturbation theory expression (see Eq. 41). States $|\alpha\rangle$ and $|\beta\rangle$ belong to the hard-core bosons subspace, and $|\gamma\rangle$ states are those which do not belong to that subspace. The first order term is straighforwardly a hard-core boson hopping into a hole since there is no other process that connects two states in the hard-core bosons manifold. Thus, it reads

$$\hat{H}_{\text{eff}}^{(1)} = -J\sum_i^{N_s}\left[\hat{a}_i^\dagger \hat{a}_{i+1} + \text{h.c.}\right]. \tag{50}$$

Note that this term takes into account the forbidden double occupation of a site due to the relation $(\hat{a}_i^\dagger)^2 = 0$.

The second order correction has both diagonal and non-diagonal terms, let us first obtain the diagonal terms. The only way to connect a state with itself through a double hopping is by having two particles in first neighboring sites and making one of them hop to the other site and back (the same process can be done with the other particle). This process requires an energy of $-2J^2/U$ and, since there are two possible processes, the prefactor is $-4J^2/U$. Thus, since such process needs two bosons to be in neighboring sites, its operator form reads

$$\hat{H}_{\text{eff}}^{(2)} = -\frac{4J^2}{U}\sum_i^{N_s} \hat{n}_i\hat{n}_{i+1}. \tag{51}$$

Non-diagonal terms are obtained by a correlated hopping process, where a boson hops to a second neighbor site due to the presence of another boson in the middle site. The energy required for this process is $-2J^2/U$. Thus this term in operator form reads

$$\hat{H}_{\text{eff}}^{(2)} = -\frac{2J^2}{U}\sum_i^{N_s} \left[\hat{a}_{i-1}^\dagger \hat{n}_i \hat{a}_{i+1} + \text{h.c.}\right]. \tag{52}$$

The number operator ensures that there is a boson in the middle site which can mediate the superexchange process. With all three terms, the whole effective Hamiltonian in operator form can be written as

$$\hat{H}_{\text{eff}} = -J\sum_i^{N_s} \left[\hat{a}_i^\dagger \hat{a}_{i+1} + \text{h.c.}\right] - \frac{4J^2}{U}\sum_i^{N_s} \hat{n}_i\hat{n}_{i+1} - \frac{2J^2}{U}\sum_i^{N_s} \left[\hat{a}_{i-1}^\dagger \hat{n}_i \hat{a}_{i+1} + \text{h.c.}\right]. \tag{53}$$

D.4 Effective Hamiltonian. Fermionic hole operators

The Hamiltonian represented by the matrix elements in Eq. 49 can be written in operator form using hole operators $\hat{h}_f^\dagger$ and $\hat{h}_f$, which create and annihilate holes that fulfill fermionic statistics. To do so, we start from the expression of Eq. 53, computed in Appendix D.3. We can rewrite the Hamiltonian with fermionic operators $\hat{c}^\dagger$ and $\hat{c}$ using the Jordan-Wigner transformation (see Eq. 5). The new Hamiltonian written with fermionic operators reads

$$\hat{H}_{\text{eff}} = -J\sum_i^{N_s} \left[\hat{c}_i^\dagger \hat{c}_{i+1} + \text{h.c.}\right] - \frac{4J^2}{U}\sum_i^{N_s} \hat{n}_i\hat{n}_{i+1} + \frac{2J^2}{U}\sum_i^{N_s} \left[\hat{c}_{i-1}^\dagger \hat{n}_i \hat{c}_{i+1} + \text{h.c.}\right]. \tag{54}$$

To follow up, we can now transform our operators again, this time from fermionic operators to hole operators, which will trivially follow the same statistics: $\hat{c}_i \leftrightarrow \hat{h}_i^\dagger$, $\hat{c}_i^\dagger \leftrightarrow \hat{h}_i$ and $\{\hat{h}_i, \hat{h}_j^\dagger\} = \delta_{i,j}$, $\{\hat{h}_i, \hat{h}_j\} = \{\hat{h}_i^\dagger, \hat{h}_j^\dagger\} = 0$, $\left(\hat{h}_i^\dagger\right)^2 = \left(\hat{h}_i\right)^2 = 0$ (we drop the subscript f for these hole operators for more clear notation). After some mathematical manipulations, the Hamiltonian written with fermionic hole operators reads

$$\begin{aligned}\hat{H}_{\text{eff}} = J\sum_i^{N_s} \left[\hat{h}_i^\dagger \hat{h}_{i+1} + \text{h.c.}\right] - \frac{4J^2}{U}N_s + \frac{8J^2}{U}\sum_i^{N_s} \hat{n}_i^h - \frac{4J^2}{U}\sum_i^{N_s} \hat{n}_i^h\hat{n}_{i+1}^h \\ -\frac{2J^2}{U}\sum_i^{N_s} \left[\hat{h}_{i+1}^\dagger \hat{h}_{i-1} + \text{h.c.}\right] + \frac{2J^2}{U}\sum_i^{N_s} \left[\hat{h}_i^\dagger \hat{h}_{i+1}^\dagger \hat{h}_{i-1}\hat{h}_i + \text{h.c.}\right],\end{aligned} \tag{55}$$

where $\hat{n}_i^h$ is the hole number operator, which counts the number of holes at site i (observe that, since $\left(\hat{h}_i^\dagger\right)^2 = 0$, the only possible values of the number operator are 0 or 1). Note that the fourth term of this Hamiltonian represents an attractive interaction between two holes (when $U > 0$). In addition, last term vanishes as long as the system has a single hole. Since we are working in the space with a single hole, the effective Hamiltonian for our specific case can finally be written as

$$\hat{H}_{\text{eff}} = J\sum_i^{N_s}\left[\hat{h}_i^\dagger\hat{h}_{i+1} + \text{h.c.}\right] - \frac{4J^2}{U}(N_s - 2) - \frac{2J^2}{U}\sum_i^{N_s}\left[\hat{h}_{i+1}^\dagger\hat{h}_{i-1} + \text{h.c.}\right]. \tag{56}$$

This Hamiltonian can be solved analytically by going to momentum space and applying the Fourier transformations

$$\begin{aligned}\hat{h}_j^\dagger &= \frac{1}{\sqrt{N_s}}\sum_q e^{-iqx_j}\hat{h}_q^\dagger,\\ \hat{h}_j &= \frac{1}{\sqrt{N_s}}\sum_q e^{iqx_j}\hat{h}_q.\end{aligned} \tag{57}$$

Hence, the effective Hamiltonian in momentum space reads

$$\hat{H}_{\text{eff}} = 2J\sum_q \hat{h}_q^\dagger\hat{h}_q\cos q + \frac{8J^2}{U}\sum_q \hat{h}_q^\dagger\hat{h}_q - \frac{4J^2}{U}N_s - \frac{4J^2}{U}\sum_q \hat{h}_q^\dagger\hat{h}_q\cos 2q. \tag{58}$$

It is straightforward to obtain the dispersion relation for the system with a single hole, which reads

$$E_{hole}^f = 2J\cos q + \frac{8J^2}{U} - \frac{4J^2}{U}N_s - \frac{4J^2}{U}\cos 2q. \tag{59}$$

It is shown that the dispersion relation for fermionic holes differs from that of bosonic holes by a sign in the linear term in J.

D.5 Shift in quasimomentum between hard-core bosons and fermions

We can see that the energy of the system treated with bosonic and fermionic holes differs on a single sign,

$$\begin{aligned}E_{hole}^f &= 2J\cos q^f + \frac{8J^2}{U} - \frac{4J^2}{U}N_s - \frac{4J^2}{U}\cos 2q^f,\\ E_{hole}^b &= -2J\cos q^b + \frac{8J^2}{U} - \frac{4J^2}{U}N_s - \frac{4J^2}{U}\cos 2q^b.\end{aligned} \tag{60}$$

Since we know that the energy spectrum should be the same, we can guess that the quasimomentum distribution for both cases is different and hence, the states have different q (that is why we made the distinction of q^b and q^f). Mathematically it is easily seen that, in order to get the same energy for both cases, it is requested $q^f = \pi \pm q^b$.

To see this in a clearer way, we can analyze the state with $N = N_s - 1$. We can write it with operators for fermions and hardcore bosons (we will write the states as plane waves in order to make them have well defined quasimomentum q):

$$
\begin{aligned}
|\psi_f\rangle &= \sum_j e^{iqx_j} \left[\hat{c}_j \prod_i^{N_s} \hat{c}_i^\dagger |0\rangle \right] \qquad x_j \equiv j, \\
|\psi_b\rangle &= \sum_j e^{iqx_j} \left[\hat{a}_j \prod_i^{N_s} \hat{a}_i^\dagger |0\rangle \right] \qquad x_j \equiv j.
\end{aligned}
\tag{61}
$$

Applying then the Jordan-Wigner transformation on the bosonic state leads to the state

$$
|\psi_b\rangle = \sum_j e^{iqj} \left[e^{i\pi \sum_{k<j} \hat{n}_k} \hat{c}_j \prod_i^{N_s} e^{i\pi \sum_{l<i} \hat{n}_l} \hat{c}_i^\dagger |0\rangle \right]. \tag{62}
$$

The second J-W exponential does not play any role since the Mott state is filled from $i = N_s$ to $i = 1$. Thus, no minus sign would be added to the state. The first exponential can be re-written as $e^{i\pi \sum_{k<j} \hat{n}_k} = e^{i\pi(j-1)}$ since all sites $k < j$ are occupied. Thus, a non-relevant global phase appears as well as a shift in quasimomentum,

$$
|\psi_b\rangle = (-1) \sum_j \left[e^{i(q+\pi)j} \hat{c}_j \prod_i^{N_s} \hat{c}_i^\dagger |0\rangle \right]. \tag{63}
$$

Hence, the difference between the state defined with hard-core bosons and fermions is a shift in quasimomentum, which results in a differing sign in the first term of the energy.

E $\hat{H}(U) = -\hat{H}(-U)$ symmetry

E.1 Bose-Hubbard Hamiltonian

The Bose-Hubbard Hamiltonian reads

$$
\hat{H} = -J \sum_i^{N_s} \left[\hat{b}_i^\dagger \hat{b}_{i+1} + \text{h.c.} \right] + \frac{U}{2} \sum_i^{N_s} \hat{n}_i (\hat{n}_i - 1). \tag{64}
$$

A sign change of the on-site interaction U would just change the second term. We can then apply the following unitary transformation to the bosonic creation and anihilayion operators, which reads

$$
\begin{aligned}
\hat{b'}_k^\dagger &= e^{-i\pi k} \hat{b}_k^\dagger, \\
\hat{b'}_k &= e^{i\pi k} \hat{b}_k.
\end{aligned}
\tag{65}
$$

Substituting the new operators in the original Hamiltonian yields a change of sign of the hopping term as long as the number of sites N_s is even for periodic boundary conditions, or the system has open boundary conditions regardless the value of N_s. Assuming one of these two conditions is fulfilled and combining both the unitary transformation and the change of sign of U, one gets

$$
\hat{H}(U) = -\hat{H}(-U). \tag{66}
$$

This result shows that, from Eq. 65, a state with quasimomentum q at a certain value of U in the system will change its quasimomentum to $q' = q - \pi$ when the on-site interaction changes its sign.

E.2 Effective Hamiltonian

The effective Hamiltonian reads

$$\hat{H}_{\text{eff}} = -J\sum_{i}^{N_s}\left[\hat{h}_i^\dagger \hat{h}_{i+1} + \text{h.c.}\right] - \frac{4J^2}{U}(N_s - 2) - \frac{2J^2}{U}\sum_{i}^{N_s}\left[\hat{h}_{i+1}^\dagger \hat{h}_{i-1} + \text{h.c.}\right]. \tag{67}$$

A sign modification of U changes the sign of the second and third terms of the Hamiltonian. We apply then a unitary transformation to the hole creation and annihilation operators,

$$\begin{aligned} \hat{h'}_k^\dagger &= e^{-i\pi k}\hat{h}_k^\dagger, \\ \hat{h'}_k &= e^{i\pi k}\hat{h}_k. \end{aligned} \tag{68}$$

Substituting the new operators in the original effective Hamiltonian yields a change of sign of the hopping term to first neighbors as long as N_s is even for periodic boundary conditions, or the system has open boundary conditions regardless the value of N_s. Assuming one of these two conditions is fulfilled and combining the unitary transformation with the sign change of U, one gets

$$\hat{H}_{\text{eff}}(U) = -\hat{H}_{\text{eff}}(-U). \tag{69}$$

This result shows that, from Eq. 68, a state with quasimomentum q at a certain value of U in the system will change its quasimomentum to $q' = q - \pi$ when the on-site interaction changes its sign.

F Time evolution

F.1 Single particle

To deal with the single particle case, let us consider the state $|0,0,0,...,0,1,0,...,0,0,0\rangle$ as the initial state of the system. To simplify the notation we will write this state as $|\psi_0\rangle$, where the subscript indicates the position where the particle is found with respect to the initial state (note that every state of the Fock basis can be uniquely written in this notation). Hence, $|0,0,0,...,1,0,0,...,0,0,0\rangle \equiv |\psi_{-1}\rangle$, $|0,0,0,...,0,0,1,...,0,0,0\rangle \equiv |\psi_1\rangle$ and so on.

We want to calculate the density of the site $i = \frac{N_s}{2}$ over time, which is written as

$$\rho_{i=\frac{N_s}{2}}(t) = \langle\psi_0(t)|\,\hat{b}_{\frac{N_s}{2}}^\dagger \hat{b}_{\frac{N_s}{2}}\,|\psi_0(t)\rangle = \langle\psi_0|\,e^{i\frac{\hat{H}t}{\hbar}}\hat{b}_{\frac{N_s}{2}}^\dagger \hat{b}_{\frac{N_s}{2}}e^{-i\frac{\hat{H}t}{\hbar}}\,|\psi_0\rangle\,. \tag{70}$$

Considering that the state $|\psi_0\rangle$ is the only state of the basis with non-vanishing density at site $i = \frac{N_s}{2}$, we can write

$$\hat{b}_{\frac{N_s}{2}}^\dagger \hat{b}_{\frac{N_s}{2}}\,|\psi_n\rangle = \hat{n}_0\,|\psi_n\rangle = \delta_{0,n}\,|\psi_0\rangle\,. \tag{71}$$

This allows us to consider $\hat{n}_0$ as a projector over the state $|\psi_0\rangle$, $\hat{n}_0 \equiv |\psi_0\rangle\langle\psi_0| = \hat{P}_0$ for our problem. Hence, the result we are looking for can be written in a more elegant way

$$\rho_{i=\frac{N_s}{2}}(t) = \langle\psi_0|\,e^{i\frac{\hat{H}t}{\hbar}}\hat{b}_{\frac{N_s}{2}}^\dagger \hat{b}_{\frac{N_s}{2}}e^{-i\frac{\hat{H}t}{\hbar}}\,|\psi_0\rangle = \left|\langle\psi_0|\,e^{-i\frac{\hat{H}t}{\hbar}}\,|\psi_0\rangle\right|^2. \tag{72}$$

We can expand the exponential in powers of $-i\frac{\hat{H}t}{\hbar}$ obtaining

$$e^{-i\frac{\hat{H}t}{\hbar}} = \sum_{n=0}^{\infty}\left(\frac{-i\hat{H}t}{\hbar}\right)^n\frac{1}{n!} = \mathbb{1} - i\frac{t}{\hbar}\hat{H} - \frac{t^2}{\hbar^2 2!}\hat{H}^2 + i\frac{t^3}{\hbar^3 3!}\hat{H}^3 + \frac{t^4}{\hbar^4 4!}\hat{H}^4 - ... \tag{73}$$

Considering that each power of $\hat{H}$ introduces a factor $-J$ and a hopping term to both right and left directions, we can apply the exponential to $|\psi_0\rangle$ obtaining

$$\begin{aligned} e^{-i\frac{\hat{H}t}{\hbar}}|\psi_0\rangle = |\psi_0\rangle + i\frac{tJ}{\hbar}(|\psi_{-1}\rangle + |\psi_1\rangle) - \frac{t^2J^2}{\hbar^2 2!}(|\psi_{-2}\rangle + 2|\psi_0\rangle + |\psi_2\rangle) \\ -i\frac{t^3J^3}{\hbar^3 3!}(|\psi_{-3}\rangle + 3|\psi_{-1}\rangle + 3|\psi_1\rangle + |\psi_3\rangle) + ... \end{aligned} \tag{74}$$

One can see that the factors of each superposition of states at each order of $\frac{Jt}{\hbar}$ are all terms in every row of the triangle of Pascal. Furthermore, they are the amount of possible paths that a boson can follow to reach the corresponding state from $|\psi_0\rangle$ by applying the Hamiltonian a certain amount of times, which is precisely the order of $\frac{tJ}{\hbar}$. Taking into account that the state of Eq. 74 will be projected into $|\psi_0\rangle$, just those terms proportional to this state will play a role. Precisely those terms can be written in a general form as $\binom{2n}{n}$ (which is the central number of every odd row of the triangle of Pascal), where n is the power of $\hat{H}$. Thus, the whole sum reads

$$\langle\psi_0|\, e^{-i\frac{\hat{H}t}{\hbar}}|\psi_0\rangle = \sum_{n=0}^{\infty}\left(\frac{itJ}{\hbar}\right)^{2n}\binom{2n}{n}\frac{1}{(2n)!} = J_0\left(\frac{2tJ}{\hbar}\right), \tag{75}$$

where J_0 is the Bessel function of first kind. Hence, following Eq. 72, the density in the central site over time will read

$$\rho_{i=\frac{N_s}{2}}(t) = J_0^2\left(\frac{2tJ}{\hbar}\right). \tag{76}$$

F.2 Single hole

We use here the same notation as in Appendix F.1. Consider the initial state $|\psi_0\rangle = |1,1,1,...,1,0,1,...,1,1,1\rangle$. The hole density over time of the central site can be written as

$$\rho_{i=\frac{N_s}{2}}(t) = \langle\psi_0(t)|\,\hat{h}^\dagger_{\frac{N_s}{2}}\hat{h}_{\frac{N_s}{2}}|\psi_0(t)\rangle = \langle\psi_0|\, e^{i\frac{\hat{H}_{\text{eff}}t}{\hbar}}\hat{h}^\dagger_{\frac{N_s}{2}}\hat{h}_{\frac{N_s}{2}}e^{-i\frac{\hat{H}_{\text{eff}}t}{\hbar}}|\psi_0\rangle, \tag{77}$$

where the Hamiltonian $\hat{H}_{\text{eff}}$ consists of a first and second neighbors hopping terms,

$$\hat{H}_{\text{eff}} = -J\sum_i^{N_s}\left[\hat{h}_i^\dagger\hat{h}_{i+1} + \text{h.c.}\right] - \frac{2J^2}{U}\sum_i^{N_s}\left[\hat{h}_{i+1}^\dagger\hat{h}_{i-1} + \text{h.c.}\right]. \tag{78}$$

Following the same procces as in Appendix F.1, we can write this result in a shorter way by using the fact that our initial state is the only eigenstate of the density operator with eigenvalue 1, while all the rest have 0 eigenvalue. This result reads

$$\rho_{i=\frac{N_s}{2}}(t) = \left|\langle\psi_0|\, e^{-i\frac{\hat{H}_{\text{eff}}t}{\hbar}}|\psi_0\rangle\right|^2 = \left|\sum_{n=0}^{\infty}\left(\frac{-it}{\hbar}\right)^n\frac{1}{n!}\langle\psi_0|\,\hat{H}^n_{\text{eff}}|\psi_0\rangle\right|^2 = \Gamma^*(t)\Gamma(t). \tag{79}$$

Following a similar procedure as in Appendix F.1, to connect a state with itself by the effective Hamiltonian to a certain power n, we have to calculate the number of closed paths that a boson can perform by applying the Hamiltonian n times [Mor22] (note these values are not anymore those from the triangle of Pascal). In the current case, the tunneling amplitude is not the same for every hopping, which requires to write the prefactor as a weight. Consider $N_{\pm 1}$ and $N_{\pm 2}$ as the number of hoppings performed to first and second neighbors respectively. The number of weighed possible paths obtained by applying the effective Hamiltonian n times can be written as [Mor22]

$$\langle \psi_0 | \hat{H}_{\text{eff}}^n | \psi_0 \rangle = f(n,J,U) = \sum_{N_{-1}=0}^{n} \sum_{N_{+1}=0}^{n} \sum_{N_{-2}=0}^{n} \sum_{N_{+2}=0}^{n} (-J)^{N_{+1}+N_{-1}} \left(\frac{-2J^2}{U}\right)^{N_{+2}+N_{-2}} \binom{n}{N_{+1}+N_{-1}} \binom{N_{+1}+N_{-1}}{N_{+1}} \binom{n-N_{+1}-N_{-1}}{N_{+2}+N_{-2}} \binom{N_{+2}+N_{-2}}{N_{+2}}. \tag{80}$$

The power n of the Hamiltonian and the fact that the paths are closed impose two conditions,

$$\begin{aligned} N_{-1}+N_{+1}+N_{-2}+N_{+2} &= n, \\ N_{+1}+2N_{+2} &= N_{-1}+2N_{-2}. \end{aligned} \tag{81}$$

With this, Eq. 80 can be simplified by writing it as a function of N_{+2}, N_{-2} and n,

$$f(n,J,U) = \sum_{N_{-2}=0}^{n/2} \sum_{N_{+2}=0}^{n/2} (-J)^{n-N_{+2}-N_{-2}} \left(\frac{-2J^2}{U}\right)^{N_{+2}+N_{-2}} \binom{n}{n-N_{+2}-N_{-2}} \binom{n-N_{+2}-N_{-2}}{\frac{n}{2}+\frac{N_{-2}-3N_{+2}}{2}} \binom{N_{+2}+N_{-2}}{N_{+2}}. \tag{82}$$

Note that with the conditions we have imposed so far we are not eliminating those solutions that have a non-integer value of $N_{\pm 1}$. To impose integer values, we need an extra rule. If the power n of the Hamiltonian is even, we need N_{+2} and N_{-2} to have the same parity, which means that their sum has to be even, $N_{+2}+N_{-2}=2k$. Nevertheless, if the power n of the Hamiltonian is odd, N_{+2} and N_{-2} need to have different parity, meaning that their sum has to be odd as well, $N_{+2}+N_{-2}=2k+1$. Then we can divide the function $\Gamma(t)$ in two sums, one for even n and another one for odd n. Since each of those sums has a power of the amplitude of the hopping to second neighbors which is $N_{+2}+N_{-2}$, we can expand the function in powers of this amplitude (we will rename it as $-\frac{2J^2}{U}=-\lambda$). While all the even powers of this amplitude will be obtained from the sum of even n, the odd powers will be obtained from the sum of odd n.

It is clear that for the power 0 (λ^0), the result should be the Bessel function. Let us check that, the factor $f(n,J,U)$ of Eq. 80 reads

$$f(n,J,U) = (-J)^n \binom{n}{\frac{n}{2}} \tag{83}$$

Note that this power in λ just takes into account even values for n, hence,

$$\Gamma(t) = \sum_{n=0}^{\infty} \left(\frac{-it}{\hbar}\right)^{2n} \frac{1}{(2n)!}(-J)^{2n}\binom{2n}{n} = J_0\left(\frac{2Jt}{\hbar}\right). \tag{84}$$

To obtain first order in λ, since $N_{+2} + N_{-2} = 1$, the powers of n that contribute are those which are odd. Hence, in the sums of Eq. 82 there will be two terms, one with $N_{+2} = 1$, $N_{-2} = 0$, and another one with $N_{+2} = 0$, $N_{-2} = 1$. These two terms have the same value since the function $f(n, J, U)$ is symmetric under the swap of N_{+2} and N_{-2}. Hence, their sum gives

$$f(n, J, U)\Big|_{N_{+2}=0,N_{-2}=1} + f(n, J, U)\Big|_{N_{+2}=1,N_{-2}=0} = \frac{2(n)!}{(\frac{n}{2}+\frac{1}{2})!(\frac{n}{2}-\frac{3}{2})!}. \tag{85}$$

Plugging this into the definition of the $\Gamma(t)$ function and taking into account that now just those n-terms which are odd must be taken into account, we get

$$\begin{aligned} &\sum_{n=0}^{\infty} \left(\frac{-it}{\hbar}\right)^{2n+1} (-J)^{2n}(-\lambda)\frac{1}{(2n+1)!}\frac{2(2n+1)!}{(n+1)!(n-1)!} = \\ &\frac{i2\lambda t}{\hbar}\sum_{n=0}^{\infty}\left(\frac{-t^2J^2}{\hbar^2}\right)^n \frac{1}{(n+1)!(n-1)!} = -\frac{i2\lambda t}{\hbar}J_2\left(\frac{2Jt}{\hbar}\right). \end{aligned} \tag{86}$$

Following this method, to obtain the second order in λ, the sum in Eq. 82 will have 3 terms, one with $N_{+2} = 2$, $N_{-2} = 0$, one with $N_{+2} = 0$, $N_{-2} = 2$, and one with $N_{+2} = 1$, $N_{-2} = 1$. Computing the first orders and after some algebraic manipulations, it is straighforward to find the pattern. The expression for $\Gamma(t)$ reads

$$\Gamma(t) = \sum_{n=0}^{\infty}\left(\frac{-i\lambda t}{\hbar}\right)^n \frac{1}{n!}\sum_{k=0}^{n}\binom{n}{k} J_{2|n-2k|}\left(\frac{2Jt}{\hbar}\right). \tag{87}$$

This expression can be described as a Taylor expansion of the exponential $\exp(-i\lambda t/\hbar)$ where each term of the expansion is weighed with a sum of Bessel functions, each of those with a weigh corresponding to its position in the triangle of Pascal. Each value of n corresponds to the row in the triangle while each value of k corresponds to the position in the row, from 0 to n. Note that while the amplitude of the hopping to second neighbors (λ) just appears in each power of the expansion, the amplitude of hopping to first neighbors (J) is just present in the argument of the Bessel functions.

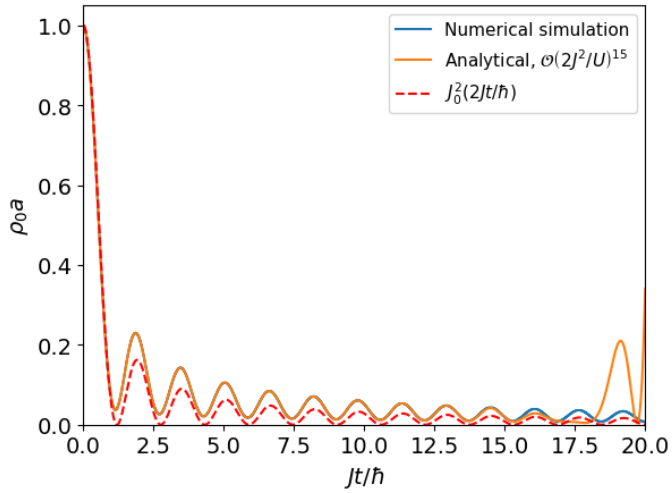

Figure 14: Comparison of the analytical result up to order 15 in $2J^2/U$ (the second neighbor hopping amplitude) in $\Gamma(t)$, the exact result obtained from the simulation by exponantiating the effective Hamiltonian to perform the time evolution, and the Bessel function $J_0^2\left(2Jt/\hbar\right)$, corresponding to the limit of the single particle case. The cases for the effective Hamiltonian have been computed for $J/U = 0.1$.